AD-A120 183 NEW MEXICO UNIV ALBUQUERQUE BUREAU OF ENGINEERING R--ETC F/G 12/1
DIAGNOSIS OF DAMAGE IN SDF STRUCTURES.(U)
MAR 82 T L PAEZ, M WANG, F D JU AFOSR-81-0086
UNCLASSIFIED CE-60(82)AFOSR-993-1 AFOSR-TR-82-0865 NL

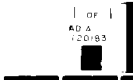

END
DATE FILMED
11-82
DTIC

AFOSR-TR- 82-0865

(6)

THE UNIVERSITY OF NEW MEXICO
COLLEGE OF ENGINEERING

BUREAU OF ENGINEERING RESEARCH

DIAGNOSIS OF DAMAGE IN SDF STRUCTURES

Scientific Report

By

Thomas L. Paez
Ming-Liang Wang
Frecerick D. Ju

Report No. CE-60(82)AFOSR-993-1
Work Performed Under AFOSR Contract No. 81-0086

Approved for public release; distribution unlimited.

DIAGNOSIS OF DAMAGE IN SDF STRUCTURES

by

Thomas L. Paez
Ming-Liang Wang
Department of Civil Engineering

Frederick D. Ju
Department of Mechanical Engineering

and

Bureau of Engineering Research
The University of New Mexico
Albuquerque, New Mexico 87131

UNM SCIENTIFIC REPORT NO. CE-60(82)AFOSR-993-1

Work Performed Under AFOSR Contract No. AFOSR-81-0086

March 1982

UNCLASSIFIED

SECURITY CLASSIFICATION OF THIS PAGE (When Data Entered)

REPORT DOCUMENTATION PAGE		READ INSTRUCTIONS BEFORE COMPLETING FORM
1. REPORT NUMBER AFOSR-TR- 82-0865	2. GOVT ACCESSION NO. AD-A120183	3. RECIPIENT'S CATALOG NUMBER
4. TITLE (and Subtitle) DIAGNOSIS OF DAMAGE IN SDF STRUCTURES		5. TYPE OF REPORT & PERIOD COVERED ANNUAL 1 Feb 81 - 28 Feb 82 6. PERFORMING ORG. REPORT NUMBER CE-60(82)AFOSR-993-1
7. AUTHOR(s) THOMAS L. PAEZ MING-LIANG WANG FREDERICK D. JU		8. CONTRACT OR GRANT NUMBER(s) AFOSR-81-0086
9. PERFORMING ORGANIZATION NAME AND ADDRESS DEPARTMENT OF CIVIL ENGINEERING UNIVERSITY OF NEW MEXICO ALBUQUERQUE, NM 87131		10. PROGRAM ELEMENT, PROJECT, TASK AREA & WORK UNIT NUMBERS 61102F 2307/C2
11. CONTROLLING OFFICE NAME AND ADDRESS AIR FORCE OFFICE OF SCIENTIFIC RESEARCH/NA BOLLING AFB, DC 20332		12. REPORT DATE March 1982 13. NUMBER OF PAGES 76
14. MONITORING AGENCY NAME & ADDRESS(if different from Controlling Office)		15. SECURITY CLASS. (of this report) Unclassified 15a. DECLASSIFICATION/DOWNGRADING SCHEDULE

16. DISTRIBUTION STATEMENT (of this Report)

Approved for Public Release; Distribution Unlimited.

17. DISTRIBUTION STATEMENT (of the abstract entered in Block 20, if different from Report)

18. SUPPLEMENTARY NOTES

19. KEY WORDS (Continue on reverse side if necessary and identify by block number)

Damage, Diagnosis, Structures, Structural Response, Structural Vibrations, Structural Dynamics, Nonlinear Response, Hysteretic Response, Random Vibration, Parameter Identification, System Identification.

20. ABSTRACT (Continue on reverse side if necessary and identify by block number)

A technique for the diagnosis of damage in hysteretic structures is developed. A hysteretic SDF system is modeled using a higher-order linear ordinary differential equation. Stochastic, dynamic inputs are generated and used to represent field inputs. The response of a hysteretic structure to each input is computed. The generated inputs and computed responses are used to identify the parameters of the higher-order linear model. Then the energy dissipated by the hysteretic structure and its linear model are computed and compared. It is shown that the energy dissipated by a hysteretic structure is accurately

DD FORM 1 JAN 73 1473 EDITION OF 1 NOV 65 IS OBSOLETE

UNCLASSIFIED

SECURITY CLASSIFICATION OF THIS PAGE (When Data Entered)

(Continued from first side)

20. estimated by the energy dissipated in its linear model, even when the measured input and response records include measurement noise. Numerical examples are presented.

TABLE OF CONTENTS

LIST OF FIGURES

LIST OF FIGURES (Continued)

LIST OF FIGURES (Concluded)

LIST OF TABLES

DIAGNOSIS OF DAMAGE IN SDF STRUCTURES

1.0 Introduction

This report summarizes the results of an investigation in the diagnosis of structural damage.

The reliability of a structure is the probability that it will survive and respond to inputs in a satisfactory manner over a preestablished period of time. If the time through which a structure is intended to survive is chosen, then the reliability of a structure can be re-estimated at various times; and the reliability may vary as a function of time. At any time, the reliability of a structure is dependent upon the class of inputs to which the structure will be subjected and the condition of the structure. If damage in a structure accumulates at a faster rate than anticipated during the initial reliability estimation, then its reliability will diminish with time. Repairs can be performed on a damaged structure to increase its reliability.

In view of the potential variability of structural reliability and the dependence of reliability on the damage level in a structure, it is desirable to know how much damage has accumulated in a structure at a given time. When damage occurs in a structure, it can appear in the form of cracks and permanent structural deformation.

An indicator of the damage which accumulates in a structure as the result of structural motion over a period of time is the energy dissipated by the structure during that time. Therefore, we wish to estimate this quantity. Particularly, it is important to estimate the energy dissipated in a structure as it responds to strong motion excitations, for this type of response causes the greatest damage. The energy dissipated by a structure responding to strong motion excitation is dissipated due to the

hysteretic behavior of the structural material. The equations governing the hysteretic structural response of a lumped mass system are second-order, nonlinear, ordinary differential equations with history-dependent stiffness terms.

In the present investigation, it is assumed that the hysteretic response of a lumped mass system is approximately governed by a higher-order, linear, ordinary differential equation. This assumption is motivated by studies summarized in the literature. For example, Wen [1]* and Baber and Wen [2,3] have used a third-order, linear, ordinary differential equation to approximately govern the response of a hysteretic single-degree-of-freedom (SDF) system to white noise and non-white stationary random inputs; and they have used a system of third-order, linear, differential equations to approximately govern the response of hysteretic multi-degree-of-freedom (MDF) structures. Their results show that the higher-order linear system provides an acceptable model for the hysteretic system. Lutes [4] used linear, third- and fourth-order equations to approximately govern the response of an SDF hysteretic system. His results show that the spectral density of the hysteretic structural response can be matched by the linear systems; in addition, the buildup of structural response in the hysteretic system can be matched by the higher-order linear systems. Another study by Wafa [5] showed that the peak response executed by a hysteretic SDF system excited by an earthquake-type input is closely predicted by a third-order, linear, equivalent system.

The purpose of the present investigation is to show that the parameters of a linear, higher-order, differential equation, approximately governing the response of a hysteretic SDF system, can be estimated using system identification techniques. The

*Numbers in parentheses refer to a list of references appended to this report.

parameter identifications will be based on measured input (forcing) and output (response) data. Parameter identification for the linear system must be attempted when the measured input and output signals are noisy, since some noise is present in all measured signals. Therefore, system identification techniques which can be used successfully in the presence of noise will be demonstrated.

The reason for pursuing the system identification study summarized in this report is to characterize the linear system equivalent to the hysteretic system in which the damage has occurred. Once the linear system parameters are known, the energy dissipated by this system can be computed. It is hoped that the energy dissipated by the higher-order, linear system is an accurate estimator of the energy dissipated by the actual hysteretic system. This study addresses the question of energy dissipated by these two types of systems.

This report covers the following subjects: 1) The system used to model a hysteretic SDF system is presented. This model is a higher-order, linear, differential equation. 2) The parameter identification technique is given. Least-squares parameter identification is used in the frequency domain and in the time domain. 3) Analysis of errors arising from the presence of noise in the measured inputs and outputs is presented. 4) Several numerical examples are summarized. 5) Discussion and conclusions are given.

2.0 Model for Hysteretic SDF System

The differential equation governing the response of a mass excited, potentially-hysteretic, single-degree-of-freedom (SDF) structure is

$$m\ddot{z} + u = f \tag{2.1}$$

where m is the structure mass, f is the forcing function, z is the displacement response of the mass, dots denote differentiation with respect to time, and u is the restoring force of the structure. In actual systems which can be realistically modeled using Equation 2.1, u can be a complicated function. When the system displacements are small, u can reasonably be taken as a linear function of the displacement and velocity; but when the displacement and velocity become large, u may be a function generating system hysteresis and whose characteristics possibly vary with time.

In analytical studies, u is modeled as a linear function of displacement and velocity when these quantities are small, and, sometimes, when they are large. When an effort is made to account for system hysteresis accurately, u is taken as a function of time and the response history. For example, when a system has bilinear hysteretic stiffness, its graph of restoring force versus system displacement might resemble the curve shown in Figure 2.1a. A column made from elasto-plastic material, with rectangular cross section, and responding in bending will have a restoring force versus displacement graph like the one shown in Figure 2.1b.

We propose that the response of a system governed by Equation 2.1 be modeled using the equations

$$m\ddot{z} + u = f$$

$$\sum_{j=0}^{M} c_j \, u^{(j)} = c_{M+1} \, \dot{z} + z \qquad (2.2)$$

where the c_j, j=0, ... M+1, are constants governing the system-restoring force characteristics, $u^{(j)}$ denotes the jth time derivative of u, and M is a constant denoting the order of approximation of the linear system to the hysteretic one. This model is

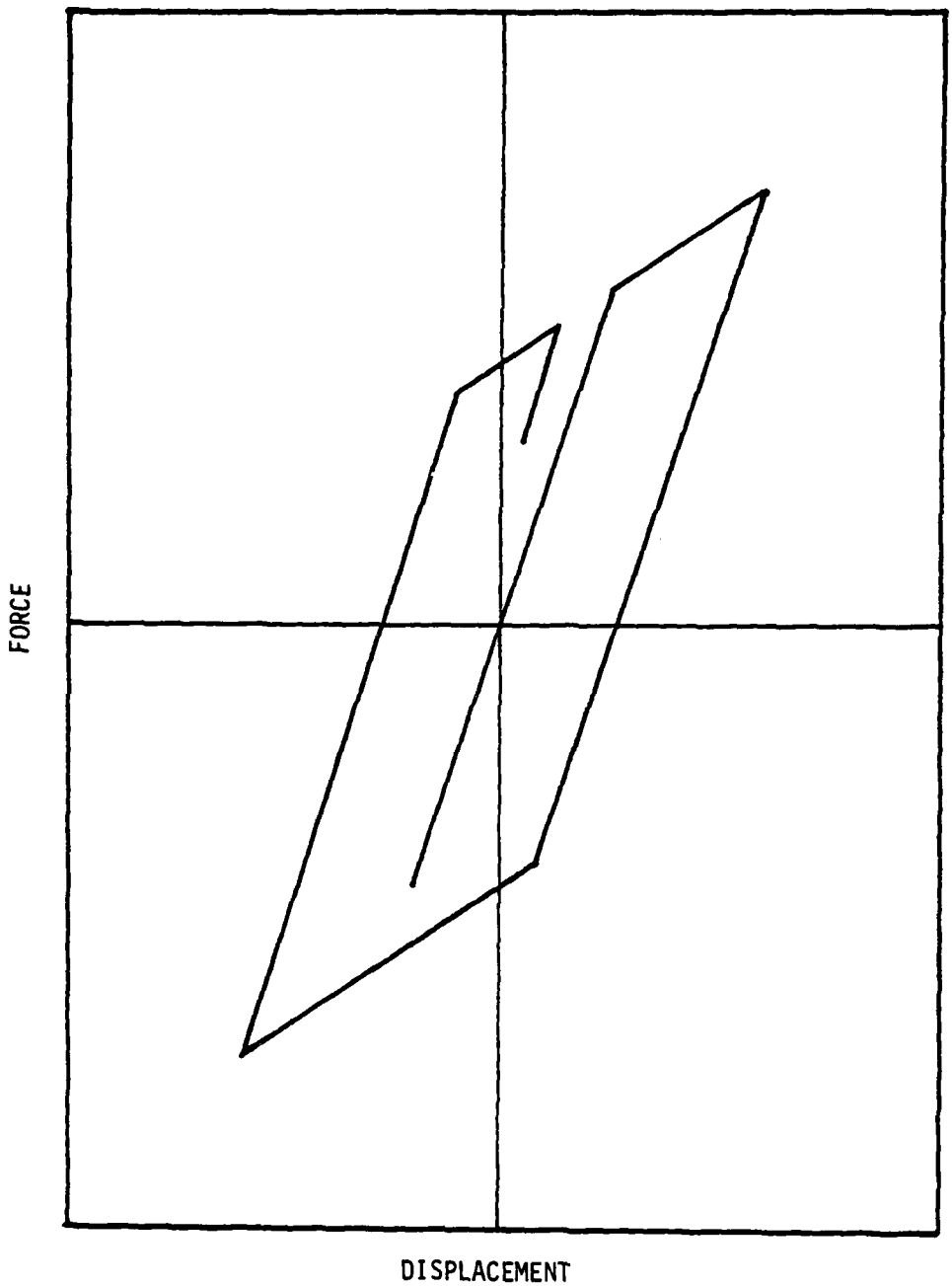

Figure 2.1a. Spring restoring force versus displacement for bilinear hysteretic structure

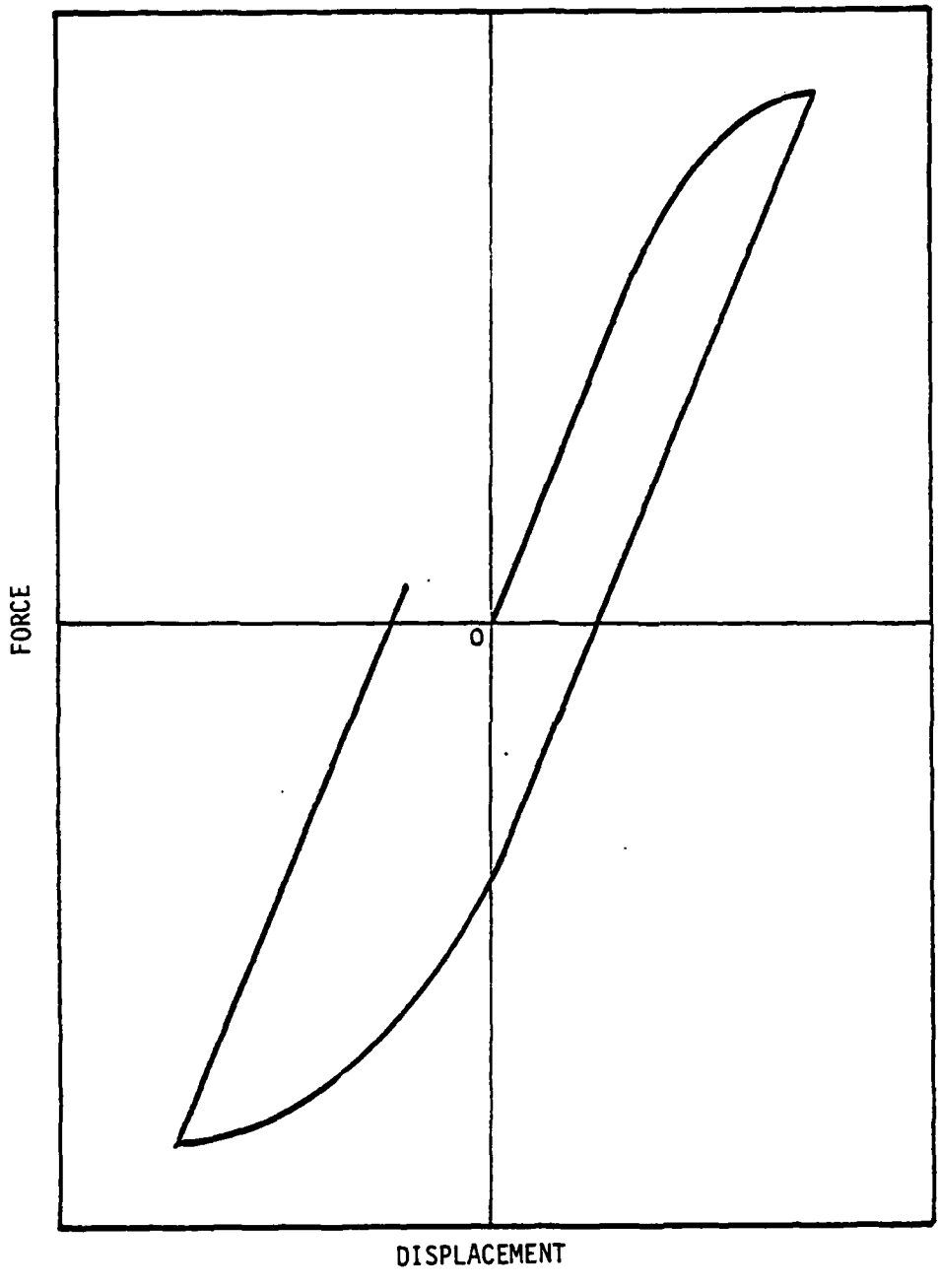

Figure 2.1b. Spring restoring force versus displacement for rectangular column in bending

chosen to represent the hysteretic system because it displays hysteresis; moreover, it is hoped that with the proper choice of c_j, j=0, ... M+1, the response of this system will accurately approximate the response of the actual system.

Note that when M is chosen to be 0, the model in Equation 2.2 becomes

$$m\ddot{z} + \frac{c_1}{c_0}\dot{z} + \frac{1}{c_0} z = f \qquad (2.3)$$

This is simply the linear differential equation which approximately governs the response of an SDF system whose response amplitude is small. The restoring force function for this system is $u = (c_1/c_0)\,\dot{z} + (1/c_0)\,z$. This system displays an energy dissipation characteristic due to viscous damping. For example, the linear system whose parameters are listed in Figure 2.2a produces the restoring force versus displacement graph shown in Figure 2.2a when the system is subjected to the harmonic force input whose form is given in Figure 2.2a. The parameters of the model in Equation 2.3 can be chosen so that the model represents the hysteretic system as well as possible, in some sense. When the response of the actual system is linear and damping is viscous, the model of Equation 2.3 perfectly represents the actual system.

When the constant M is chosen as 1 in Equation 2.3, the model becomes

$$m\ddot{z} + u = f$$

$$c_0 u + c_1 \dot{u} = c_2 \dot{z} + z \qquad (2.4)$$

The restoring force is the solution of the second equation. This system can display an energy-dissipation characteristic. For

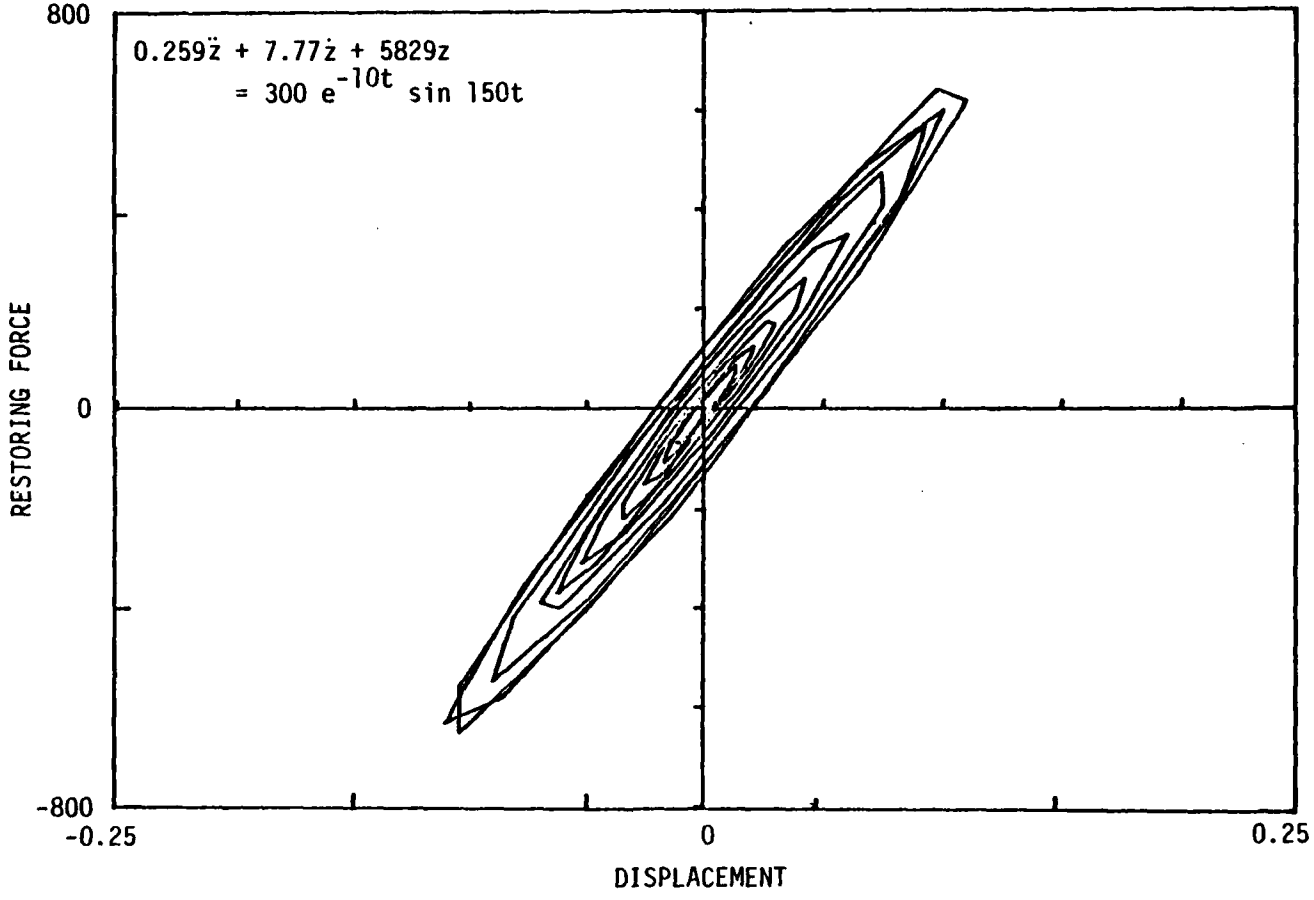

Figure 2.2a. Total restoring force versus displacement for second-order system

example, the linear system whose parameters are listed in Figure 2.2b produces the restoring force versus displacement graph shown in Figure 2.2b when the system is excited by the harmonic input whose form is given in Figure 2.2b. The parameters of the system in Equation 2.4 can be chosen so that the model represents a hysteretic system as well as possible, in some sense. When the actual system response is linear and the system has viscous damping, we anticipate that $c_1 = 0$.

It is anticipated that as the order, M, of the model in Equation 2.2 is increased, the response of a hysteretic system can be matched with increasing accuracy. However, for practical reasons involving estimation accuracy for system parameters, very high order linear system models cannot be used to simulate hysteretic system behavior.

Before considering the problem of parameter estimation for the system of Equation 2.2, note that we anticipate calculating a set of parameters with values in a specific range. For example, when M=0 and Equation 2.3 is the model for system response, we anticipate finding values $1/c_0 > 0$ and $c_1/c_0 > 0$ (i.e., $c_0 > 0$ and $c_1 > 0$). These values guarantee that the model has positive stiffness and damping, as we know the real system must. When M=1 and Equation 2.4 models the system response, we anticipate finding values $c_0 > 0$, $c_1 > 0$, and $c_2 > 0$. These values guarantee that the model response will be stable.

The energy dissipated by the systems described in this section can be computed using Equation 2.1 or 2.2. In the terms of Equation 2.1, the energy dissipated by a system is

$$E_D = \int_{z(0)}^{z(T)} u \, dz \qquad (2.5)$$

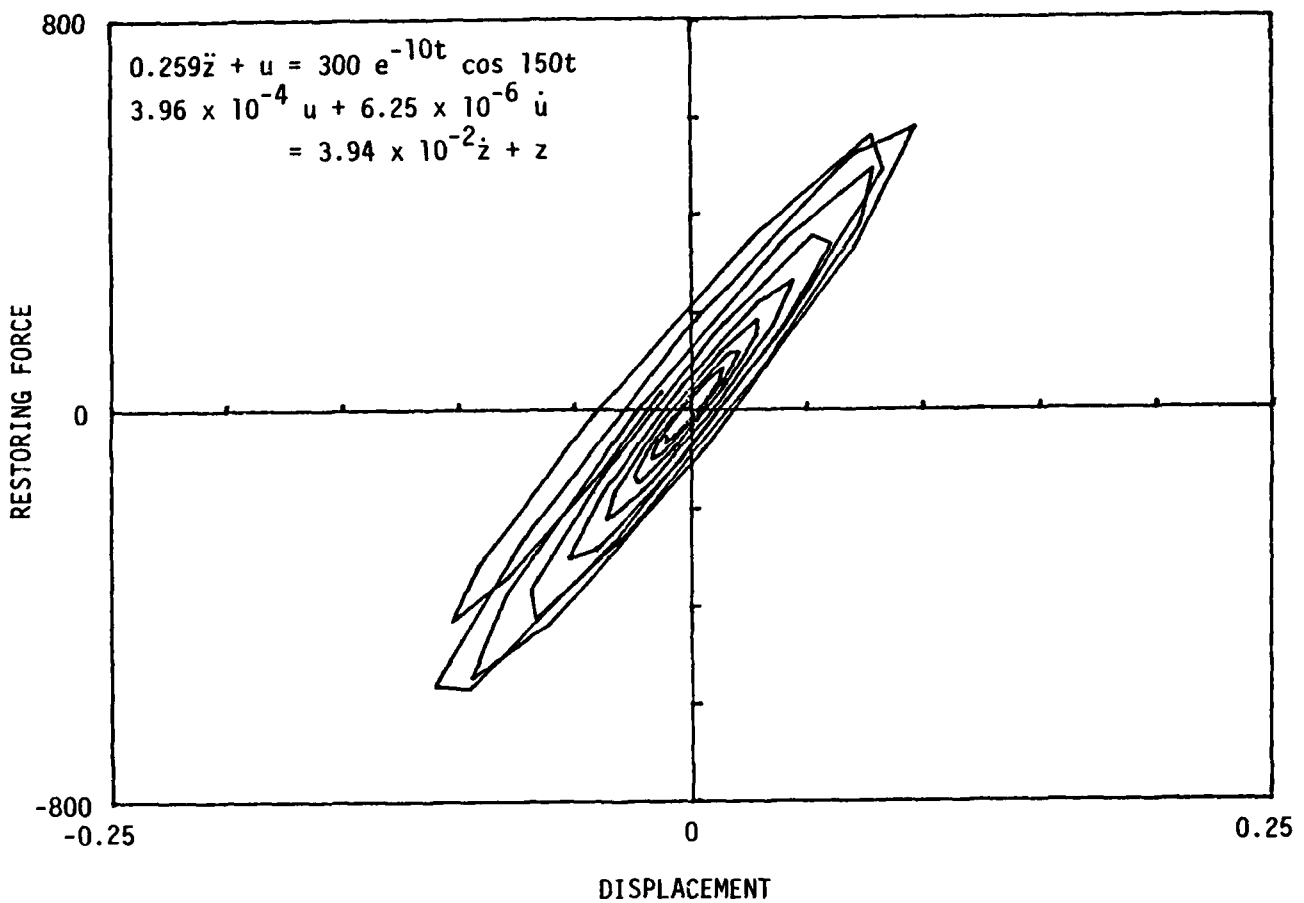

Figure 2.2b. Total restoring force versus displacement for third-order system

where z(0) is the system displacement at time 0, z(T) is the system displacement at time T, and T is the time through which the energy computation is executed. This formula provides the area enclosed in the hysteresis loops generated by the system response. For example, Equation 2.5 could be used to compute the area enclosed by the hysteresis loop of Figure 2.1b. This equation can be transformed into terms more convenient for computation. Note that the integral of Equation 2.5 is written in terms of the displacement variable z. The variable of integration can be transformed to a time variable yielding the following expression.

$$E_D = \int_0^T u \dot{z} \, dt \qquad (2.5a)$$

Finally, Equation 2.1 can be used above to obtain

$$E_D = \int_0^T (f - m\ddot{z}) \dot{z} \, dt \qquad (2.5b)$$

When the input and response for an SDF system are measured, Equation 2.5b can be used to directly compute the energy dissipated by a system. When the response is computed, for example by solving Equations 2.4, then the input and system parameters are used to find z and its derivatives. The input, f, and computed response, z, are used in Equation 2.5b to determine the energy dissipated.

Numerical examples where we compute the parameters of linear systems equivalent to bilinear, hysteretic systems are presented in Section 5. In these examples, the energy dissipated by each system is computed and the results are compared.

3.0 Identification of Parameters

We now consider the problem of parameter identification for the linear model for hysteretic single-degree-of-freedom (SDF) systems introduced in the last section. Both the time and frequency domain approaches to the problem of parameter identification are outlined. We consider the parameter identification both when noise is and is not present in the measured data.

Measured input and output data from a structural system are used to estimate the system parameters. It is assumed that these data are available. To begin with, we assume that no noise is present in the measured data. Later, modifications are made to permit the inclusion of noise. The input, or forcing function, data are available in discrete form and are denoted f_ℓ, $\ell=0$, ... $n-1$. The output, or system response, data are available in discrete form and are denoted $\ddot{z}_\ell$, $\ell=0$, ... $n-1$. It is assumed that the input and output signals have been sampled at times $t_\ell = \ell\Delta t$, $\ell=0$, ... $n-1$. Note that measured response data are assumed to be given as accelerations; this is realistic since structural response acceleration is often the quantity measured during an experiment.

The approaches to parameter identification developed in this section do not require that the measured data be indexed by time. Any sampled sets f_ℓ and $\ddot{z}_\ell$, $\ell=0$, ... $n-1$ can be used. However, since the present applications come from the field of structural dynamics, we will refer to signals sampled in time.

The model established in Equation 2.2 is repeated here; it is

$$m\ddot{z} + u = f$$

$$\sum_{j=0}^{M} c_j \, u^{(j)} = c_{M+1} \, \dot{z} + z \qquad (3.1)$$

When the first of these equations is solved for u and the resulting expression is used in the second equation, we obtain

$$\frac{1}{c_0} z + \frac{c_{M+1}}{c_0} \dot{z} + \sum_{j=1}^{M} \frac{c_j}{c_0} (-f^{(j)} + mz^{(j+2)}) = f - m\ddot{z} \tag{3.2}$$

where $f^{(j)}$ is the jth derivative of f, and $z^{(j+2)}$ is the (j+2)th derivative of z. (This particular arrangement is chosen since c_0 should never be 0 for the systems under consideration.) The notation in this equation can be simplified by taking

$$a_0 = \frac{1}{c_0}, \; a_1 = \frac{c_{M+1}}{c_0}, \; a_{j+1} = \frac{c_j}{c_0}, \; j=1, \; \ldots \; M. \tag{3.3}$$

The equation governing motion of the system becomes

$$a_0 z + a_1 \dot{z} + \sum_{j=1}^{M} a_{j+1} (-f^{(j)} + mz^{(j+2)}) = f - m\ddot{z}. \tag{3.4}$$

This equation can be used, along with the measured input and response data, to identify the parameters a_j, j=0, ... M+1. When these are known, Equation 3.3 can be used to find the c_j, j=0, ... M+1.

3.1 Time Domain Approach I

Let z_ℓ, $\dot{z}_\ell$, and $z_\ell^{(j)}$, ℓ=0, ... n-1, be, respectively, the response displacement, velocity and jth derivative of the displacement at time, t_ℓ, ℓ=0, ... n-1. Let f_ℓ and $f_\ell^{(j)}$, ℓ=0, ... n-1, be the force at time t_ℓ, ℓ=0, ... n-1. Assume that all required integrals and derivatives of f_ℓ and $\ddot{z}_\ell$ can be

obtained, exactly. Then Equation 3.4 can be written at time t_ℓ as

$$a_0 z_\ell + a_1 \dot{z}_\ell + \sum_{j=1}^{M} a_{j+1}(-f_\ell^{(j)} + m z_\ell^{(j+2)}) = f_\ell - m\ddot{z}_\ell, \quad \ell=0, \ldots n-1 \tag{3.5}$$

The notation in this equation can be simplified by defining

$$\{z_\ell\} = (z_\ell \quad \dot{z}_\ell \quad -\dot{f}_\ell + m\dddot{z}_\ell \quad \ldots \quad -f_\ell^{(M)} + m z_\ell^{(M+2)})^T, \quad \ell=0, \ldots n-1 \tag{3.6a}$$

$$\{a\} = (a_0 \quad a_1 \quad \ldots \quad a_{M+1})^T \tag{3.6b}$$

where the T superscript refers to matrix transposition. Use of these expressions in Equation 3.5 yields the relation

$$\{z_\ell\}^T \{a\} = f_\ell - m\ddot{z}_\ell \qquad \ell=0, \ldots n-1 \tag{3.7}$$

This is the equation governing the linear system response at time t_ℓ.

The notation can be further simplified by defining

$$[Z_f] = \begin{bmatrix} \{z_0\}^T \\ \{z_1\}^T \\ \vdots \\ \{z_{n-1}\}^T \end{bmatrix}, \quad \{f_z\} = \begin{Bmatrix} f_0 - m\ddot{z}_0 \\ f_1 - m\ddot{z}_1 \\ \vdots \\ f_{n-1} - m\ddot{z}_{n-1} \end{Bmatrix} \tag{3.8}$$

Using these expressions, the sequence of Equation 3.7, for $\ell=0$, ... n-1, can be written

$$[Z_f]\{a\} = \{f_z\} \tag{3.9}$$

This equation governs the linear system response at all times.

When 1) the mechanical system from which the data were measured is truly linear, 2) there is no noise in the data measurements, and 3) the derivatives and integrals of f_ℓ and $\ddot{z}_\ell$, ℓ=0, ... n-1, are known exactly, Equation 3.9 can be satisfied exactly by the measured data and a set of coefficients, a_j, j=0, ... M+1. Otherwise, the left-hand side of Equation 3.9 will not exactly equal the right-hand side at every time, t_ℓ. We define the error vector as follows.

$$\{\varepsilon\} = (\varepsilon_0 \quad \varepsilon_1 \quad \cdots \quad \varepsilon_{n-1})^T \tag{3.10}$$
$$= [Z_f]\{a\} - \{f_z\}$$

The elements ε_ℓ, ℓ=0, ... n-1, quantify the data nonlinearity, the measurement noise, and the inaccuracy of the derivatives and integrals of $\ddot{z}_\ell$ and f_ℓ, as a function of the system parameters, $\{a\}$.

An overall measure of the lack of fit of the measured data to the model in Equation 3.9 is established in the parameter

$$\varepsilon^2 = \{\varepsilon\}^T\{\varepsilon\} = (\{a\}^T[Z_f]^T - \{f_z\}^T)\,([Z_f]\{a\} - \{f_z\}) \tag{3.11}$$

This is referred to as the squared error between the measured data and the system model. This error can be minimized through the proper choice of the parameter vector $\{a\}$. The vector $\{a\}$ which minimizes ε^2 is

$$\{a\} = ([Z_f]^T[Z_f])^{-1}\,[Z_f]^T\{f_z\} \tag{3.12}$$

(See, for example, Reference 6.) The parameter vector chosen above is the best estimate of the system parameters in a least square sense.

If the quantity, ε^2/n, is small relative to the signal difference, $f_\ell - m\ddot{z}_\ell$, $\ell=0, \ldots n-1$, then the model of Equation 3.4 with parameters obtained using Equation 3.12 accurately represents the measured system. If this is not true, then the model of Equation 3.4 is inadequate.

ε^2 will equal zero if the measured system data are noise free, the system is linear, and the computed derivatives and integrals of the data are exact. Failure to meet any one or more of these requirements will cause ε^2 to be nonzero. In practice, the parameter identification procedure outlined above can only be used effectively when there is little or no noise in the measurements, the system is nearly linear, and the integrals and derivatives of $\ddot{z}$ and f can be obtained accurately. The method is particularly effective when the parameter M is set to 0. However, when noise is present and M=1, the procedure loses accuracy since derivatives of $\ddot{z}$ and f are required. Particularly, the functions $\dddot{z}$ and $\dot{f}$ must be estimated. If the measured raw data, $\ddot{z}_\ell$ and f_ℓ, $\ell=0, \ldots n-1$, are used directly to obtain these estimates through numerical differentiation, the estimates of $\dddot{z}$ and $\dot{f}$ may be very poor due to amplification of the effects of noise and inaccuracy of numerical differentiation. In view of this, alternate procedures for parameter identification in the presence of noise must be established.

It is possible to retain a time domain approach in the parameter estimation problem. For example, the signals $\ddot{z}_\ell$ and f_ℓ, $\ell=0, \ldots n-1$ can be smoothed prior to the taking of derivatives. Smoothing can be accomplished through the use of digital filters; or the governing Equation 3.4 can be integrated M times

before applying the identification procedure. Then no numerical derivatives are required. Alternately, a frequency domain approach can be used. This eliminates the necessity to directly differentiate measured data. In the present study, we pursue the approach using the integrated equations of motion and the frequency domain approach. First, we consider the time domain approach using the integrated equations of motion.

3.2 Time Domain Approach II

Consider again Equation 3.4. That equation establishes the assumed form for the governing equation of motion of a hysteretic SDF system. The direct use of that equation in a parameter identification scheme requires the calculation of $z^{(M+2)}(t)$, the Mth derivative of $\ddot{z}(t)$. The numerical computation of derivatives is an operation which is generally sensitive to the presence of noise in measured signals; therefore, we employ the following procedure. Integrate both sides of Equation 3.4 M times. We obtain

$$a_0 y_M + a_1 y_{M-1} + \sum_{j=1}^{M} a_{j+1} \left(-g_{M-j} + m y_{M-j-2}\right) = g_M - m y_{M-2} \tag{3.13}$$

where $y_{-2}(t) = \ddot{z}(t)$

$$y_j(t) = \int_0^t y_{j-1}(\tau)\, d\tau \qquad j=-1, \ldots M$$

$$g_0(t) = f(t)$$

$$g_j(t) = \int_0^t g_{j-1}(\tau)\, d\tau \qquad j=1, \ldots M.$$

It is assumed that the initial values of $z(t)$ and $f(t)$ and their derivatives are zero. Equation 3.13 involves $\ddot{z}(t)$ and its first M+2 integrals, and $f(t)$ and its first M integrals. When $\ddot{z}(t)$ and $f(t)$ are measured, these can be calculated numerically.

A parameter identification can now be executed using Equation 3.13. As before, it is assumed that $\ddot{z}(t)$ and $f(t)$ have been measured at discrete times, $t_\ell = \ell\Delta t$, $\ell=0, \ldots n-1$. The integrals of $\ddot{z}(t)$ and $f(t)$ can be directly computed at the times t_ℓ. At time $t=t_\ell$, $y_j(t)$ is denoted $y_{j,\ell}$, $g_j(t)$ is denoted $g_{j,\ell}$, and Equation 3.13 becomes

$$a_0 y_{M,\ell} + a_1 y_{M-1,\ell} + \sum_{j=1}^{M} a_{j+1}(-g_{M-j,\ell} + m y_{M-j-2,\ell}) = g_{M,\ell} - m y_{M-2,\ell}$$

$$\ell=0, \ldots n-1 \qquad (3.14)$$

This equation governs the SDF system at each time t_ℓ. The notation for the collection of equations described in 3.14 can be simplified by defining the matrices

$$\{a\} = (a_0 \;\; a_1 \;\; \cdots \;\; a_{M+1})^T \qquad (3.15a)$$

$$[Z_f] = \begin{bmatrix} y_{M,0} & y_{M-1,0} & (-g_{M-1,0} + m y_{M-3,0}) & \cdots & (-g_{0,0} + m y_{-2,0}) \\ y_{M,1} & y_{M-1,1} & (-g_{M-1,1} + m y_{M-3,1}) & & (-g_{0,1} + m y_{-2,1}) \\ \vdots & \vdots & \vdots & & \vdots \\ y_{M,n-1} & y_{M-1,n-1} & (-g_{M-1,n-1} + m y_{M-3,n-1}) & \cdots & (-g_{0,n-1} + m y_{-2,n-1}) \end{bmatrix} \qquad (3.15b)$$

$$\{f_z\} = ((g_{M,0} - m y_{M-2,0}) \; (g_{M,1} - m y_{M-2,1}) \; \cdots \; (g_{M,n-1} - m y_{M-2,n-1}))^T \qquad (3.15c)$$

In terms of these matrices, Equation 3.14 can be expressed

$$[Z_f]\{a\} = \{f_z\} \tag{3.16}$$

This equation has the same form as that used in the parameter identification problem for Equation 3.4, but the matrices $[Z_f]$ and $\{f_z\}$ have been defined differently. When 1) a physical system is exactly governed by the (M+2)th order Equation 3.1, 2) there is no noise in the measurements of $\ddot{z}(t)$ and $f(t)$, and 3) the integrals of $\ddot{z}(t)$ and $f(t)$ are computed exactly, Equation 3.16 can be satisfied exactly by the measured data and a collection of coefficients, a_j, $j=0, \ldots M+1$. However, when these requirements are not satisfied, Equation 3.16 will not hold, exactly. Then the equation

$$\{\varepsilon\} = [Z_f]\{a\} - \{f_z\} \tag{3.17}$$

will hold, where $\{\varepsilon\}$ is an error vector which reflects the degree to which the above requirements are not satisfied. As before, the sum of the squares of the components in $\{\varepsilon\}$ is minimized by choosing

$$\{a\} = ([Z_f]^T[Z_f])^{-1}\,[Z_f]^T\{f_z\} \tag{3.18}$$

When the elements in $\{\varepsilon\}$ are relatively small, Equation 3.1 provides a satisfactory model for the system under consideration and the vector $\{a\}$ includes the parameters of that model.

The advantage to the present approach to parameter identification is that the derivatives of $\ddot{z}(t)$ and $f(t)$ need not be computed via numerical differencing. This is a practical improvement since all measured signals contain at least some noise. Beyond this, the operation of numerical differencing introduces

so much inaccuracy into a computation that parameter identification is difficult, even when the signals contain no noise. The use of Equation 3.13 replaces the requirement for differentiation with an integration requirement. When the measured signals are noisy, their integrals are influenced by the presence of noise; but the noise influence is less than in the case of differentiation. In Section 4, the effect of noise on parameter identification will be discussed.

3.3 Frequency Domain Approach

The final approach we will consider for the identification of the parameters of Equation 3.4 is a frequency domain approach. Consider Equation 3.4. Both sides can be Fourier transformed to obtain

$$a_0 Z(w) + a_1 iwZ(w) + \sum_{j=1}^{M} a_{j+1} \left(-(iw)^j F(w) + m(iw)^{j+2} Z(w)\right)$$

$$= F(w) + mw^2 Z(w) \qquad -\infty < w < \infty \qquad (3.19)$$

where $Z(w) = \int_{-\infty}^{\infty} z(t)\, e^{-iwt} dt \qquad -\infty < w < \infty$

$$F(w) = \int_{-\infty}^{\infty} f(t)\, e^{-iwt} dt \qquad -\infty < w < \infty$$

are the Fourier transforms of z(t) and f(t), respectively. This equation can be rearranged by grouping the coefficients of Z(w) and F(w), then combining Z(w) and F(w) on one side of the equation.

$$\frac{-mw^2 + a_0 + a_1(iw) + m\sum_{j=1}^{M} a_{j+1}(iw)^{j+2}}{1 + \sum_{j=1}^{M} a_{j+1}(iw)^{j}} = \frac{F(w)}{Z(w)}, \qquad -\infty < w < \infty$$

(3.20)

Finally, each side of the equation can be multiplied by its complex conjugate to yield the modulus squared.

$$\frac{\left|-mw^2 + a_0 + a_1(iw) + m\sum_{j=1}^{M} a_{j+1}(iw)^{j+2}\right|^2}{\left|1 + \sum_{j=1}^{M} a_{j+1}(iw)^{j}\right|^2} = \frac{|F(w)|^2}{|Z(w)|^2}, \qquad -\infty < w < \infty$$

(3.21)

When this expression is evaluated at $w = w_k$, the result is

$$\frac{\left|-mw_k^2 + a_0 + a_1(iw_k) + m\sum_{j=1}^{M} a_{j+1}(iw_k)^{j+2}\right|^2}{\left|1 + \sum_{j=1}^{M} a_{j+1}(iw_k)^{j}\right|^2} = \frac{|F_k|^2}{|Z_k|^2} = Q_k, k=0,..\frac{n}{2}$$

(3.22)

where $|F_k|^2/|Z_k|^2$ has been set equal to Q_k. It is assumed that the estimates for the Fourier transforms of $\ddot{z}(t)$ and $f(t)$ can be obtained by using the discrete Fourier transform (DFT) of $\ddot{z}_\ell$

and f_ℓ, $\ell=0, \ldots n-1$. Then these estimates will be available at the frequencies $w_k = 2\pi k/n\Delta t$, $k=0, \ldots n/2$. The DFT can be efficiently obtained using the fast Fourier transform (FFT) procedure. (See, for example, Reference 7). The DFT of z_ℓ, $\ell=0, \ldots n-1$, is assumed to be $-w_k^2 Z_k$, $k=0, \ldots n/2$. Z_k and F_k, $k=0, \ldots n/2$, represent the DFTs of $z(t)$ and $f(t)$ at frequencies w_k, $k=0, \ldots n/2$.

When 1) the system under consideration is linear and or order M+2, 2) all measurements are noise free, and 3) the DFTs of $\ddot{z}_\ell$ and f_ℓ, $\ell=0, \ldots n-1$ used in Equation 3.22 are exact, Equation 3.22 can be satisfied exactly by the measured data and a set of coefficients, a_j, $j=0, \ldots M+1$. When these requirements are not satisfied, Equation 3.22 cannot be precisely satisfied. In this latter case, we consider the equation

$$\frac{\left| -mw_k^2 + a_0 + a_1(iw_k) + m\sum_{j=1}^{M} a_{j+1}(iw_k)^{j+2} \right|^2}{\left| 1 + \sum_{j=1}^{M} a_{j+1}(iw_k)^j \right|^2} = Q_k + \varepsilon_k, \quad k=0,\ldots\frac{n}{2} \tag{3.23}$$

On the right-hand side ε_k is an error term. This term measures the degree to which the model of Equation 3.4 represents or fails to represent the measured data, when the measured data are used to compute F_k and Z_k, $k=0, \ldots n/2$. We wish to find the coefficients a_j, $j=0, \ldots M+1$, which minimize the ε_k, $k=0, \ldots n/2$. This can be accomplished using a least-squares criterion where a sum $\sum\varepsilon_k^2$ is minimized. This can be done numerically by searching through the space of (M+2)-tuples created by the coordinates $a_0, \ldots a_{M+1}$. For example, a gradient search technique can be used to find the minimum. When M is chosen as 0 or 1 and

when the system to be analyzed has a response which is only moderately nonlinear, then a simpler technique for choosing the best a_j, j=0, ... M+1, is available. Consider first the case where M=0. When M is chosen as zero, Equation 3.4 becomes the equation of a linear, second-order, SDF system. The equation to be used in the parameter identification, Equation 3.23, can be written

$$\left|-mw_k^2 + a_0 + a_1\, iw_k\right|^2 = Q_k + \varepsilon_k,\ k=0,\ \ldots\ n/2 \qquad (3.24)$$

The left side of the expression can be expanded to yield

$$(a_0 - mw_k^2)^2 + (a_1 w_k)^2 = Q_k + \varepsilon_k,\ k=0,\ \ldots\ n/2 \qquad (3.25)$$

The functional expression on the left-hand side assumes its minimum when w takes the value

$$w = \left[\frac{1}{m}\left(a_0 - \frac{a_1^2}{2m}\right)\right]^{1/2} \qquad (3.26)$$

Note from Equation 3.4 that a_0 is the equivalent stiffness and a_1 is the equivalent damping for a system whose Equation 3.4 model uses M=0. In view of this, whenever the equivalent damping factor is much less than 1 (say less than 0.2), $a_1^2/2m$ is small compared to a_0. (This will be true in most cases.) In this case, a_0 can be estimated by noting the frequency where $Q_k + \varepsilon_k$, k=0, ... n/2 is a minimum. Denote this frequency w_m and use it in Equation 3.25 to show that

$$a_0 = mw_m^2 \qquad (3.27)$$

To obtain improved accuracy, the frequency where $Q_k + \varepsilon_k$, k=0, ... n/2 is a minimum can be estimated by using the least-squares

approach to fit a parabola to the values $Q_k + \varepsilon_k$ near the characteristic frequency, w_m. The parameters of this parabola can be used to determine the frequency where $Q_k + \varepsilon_k$ is a minimum. Estimation of the constant a_0 by any means must assume that no quality in ε_k, k=0, ... n/2, will tend to move the minimum value of Q_k, k=0, ... n/2, in a systematic way. The general character of ε_k, k=0, ... n/2, will be discussed and modeled in Section 4.

The motivation for using the above analysis to estimate a_0 is clarified by the following considerations. The characteristics of an SDF system are reflected in the system behavior at all frequencies but are best interpreted from its behavior near the characteristic frequency. (For strictly linear response, we would refer to the natural frequency, but the response considered here is not always linear.) The frequency band including the characteristic frequency is that band where the system amplifies the response, and in this band the values of Q_k, k=0, ... n/2, form a trough. This is the reason why the minimum value of $Q_k + \varepsilon_k$, k=0, ... n/2, is considered, above.

The estimated value of a_0 can now be used in Equation 3.25 to obtain

$$m^2(w_m^2 - w_k^2)^2 + (a_1 w_k)^2 = Q_k + \varepsilon_k, \quad k=0, \ldots n/2 \quad (3.28)$$

Now, in order to estimate a_1, we can employ a least-squares criterion. Specifically, we solve Equation 3.28 for ε_k, square this expression, and sum over all or part of the values of k. The resulting expression is denoted ε^2. This quantity is minimized with respect to a_1^2 by differentiating ε^2 with respect to a_1^2, equating the result to zero, and solving for a_1. The operations listed above yield the result

$$a_1 = \{(\sum_k w_k^4)^{-1} \sum_k [Q_k - m^2(w_m^2 - w_k^2)^2]w_k^2\}^{1/2} \tag{3.29}$$

The sums in Equation 3.29 are listed simply as sums over k. In the identification process, these sums should be taken over those frequencies near the characteristic frequency of the SDF system. These are the frequencies where the ratio $|F_k|^2/|Z_k|^2$ best characterizes the properties of the SDF system. For example, the values of k used in the analysis might be chosen as those corresponding to the frequencies, w_k, falling in the interval which is twice the bandwidth of the SDF system under consideration. Of course, this band of frequencies will not be precisely known since the system parameters have not been identified. However, it can be estimated as the frequency band (w_{k_1}, w_{k_2}). w_{k_1} is the lower frequency where $|F_{k_1}|^2/|Z_{k_1}|^2$ is about five times as great as the *minimum value of* $|F_k|^2/|Z_k|^2$. w_{k_2} is the higher frequency where $|F_{k_2}|^2/|Z_{k_2}|^2$ is about 5 times as great as the minimum value of $|F_k|^2/|Z_k|^2$.

The constants a_0 and a_1, expressed in Equations 3.27 and 3.29 provide the parameters for a second-order model for an SDF system. This model is the best available in a least-squares sense. Note again that the means used to obtain a_0 assumes relatively low damping.

Some may consider it undesirable or inaccurate to model a hysteretic SDF system using a second-order, linear ordinary differential equation, as we do with Equation 3.4 when M=0. With the hope of obtaining improved accuracy, we can model the SDF system under consideration using Equation 3.4 with M=1. Note first, though, that 1) improved accuracy in every sense may not be obtained using M=1. This is, using M=1 in Equation 3.4 only

guarantees that the parameters a_j, j=0,1,2 will yield a more accurate match between the motion response of the model and the measured response; the energy dissipation characteristics of the model system may not be more accurate. 2) The linear viscous damping term used in most linear system analyses does not precisely model real system behavior, even when the real system has small displacements. Yet, linear viscous damping is freely used in analyses.

When M is chosen as 1 in Equation 3.4, the formula to be used in the parameter identification is Equation 3.23 with M=1. This is

$$\frac{\left|-mw_k^2 + a_0 + a_1(iw_k) + ma_2(iw_k)^3\right|^2}{\left|1 + a_2(iw_k)\right|^2} = Q_k + \varepsilon_k, \quad k=0, \ldots n/2. \tag{3.30}$$

The numerator and denominator can be expanded on the left side to obtain

$$\frac{(a_0 - mw_k^2)^2 + w_k^2(a_1 - mw_k^2 a_2)^2}{1 + (a_2 w_k)^2} = Q_k + \varepsilon_k, \quad k=0, \ldots n/2. \tag{3.31}$$

When a_2 is small compared to the characteristic frequency, w_m of the SDF system (say $a_2 \leq 0.3\ w_m$), the $(a_2 w_k)^2$ term in the denominator can be neglected. This is usually the case when nonlinear deformations are not too large. When a_1 and a_2 are small compared to a_0 (which is usually the case) the minimum of the left-hand side occurs near the frequency

$$w = \sqrt{\frac{a_0}{m}} \tag{3.32}$$

We find this frequency by scanning $Q_k + \varepsilon_k$, k=0, ... n/2, or by using the curve fitting technique discussed above. This frequency is denoted w_m. In terms of w_m, a_0 can be written

$$a_0 = m w_m^2 \tag{3.33}$$

This expression and the previous assumptions can be used in Equation 3.31 to obtain

$$m^2(w_m^2 - w_k^2)^2 + w_k^2(a_1 - m w_k^2 a_2)^2 = Q_k + \varepsilon_k, \quad k=0, \ldots n/2 \tag{3.34}$$

When $m w_m^2 a_2$ is relatively small compared to a_1, the second term on the left side of Equation 3.34 can be expanded, and the $m^2 w_k^4 a_2^2$ term can be neglected. This is possible when the amount of yielding in the system to be modeled is not too great. The result of this operation is

$$m^2(w_m^2 - w_k^2)^2 + w_k^2(a_1^2 - 2m w_k^2 a_1 a_2) = Q_k + \varepsilon_k, \quad k=0, \ldots n/2 \tag{3.35}$$

Finally, we can set

$$a_1^2 = b_1 \text{ and } a_1 a_2 = b_2 \tag{3.36}$$

to obtain

$$w_k^2(b_1 - 2m w_k^2 b_2) - (Q_k - m^2(w_m^2 - w_k^2)^2) = \varepsilon_k, \quad k=0, \ldots n/2 \tag{3.37}$$

The system parameters, a_1 and a_2, can now be identified as those which minimize the sum of the squares of the ε_k terms in Equation 3.37.

A notational simplification can be achieved for the sequence of Equations 3.37 by defining

$$\{b\} = (b_1 \quad b_2)^T \tag{3.38a}$$

$$[X_1] = \begin{bmatrix} w_{k_1}^2 & -2mw_{k_1}^4 \\ w_{k_1+1}^2 & -2mw_{k_1+1}^4 \\ \vdots & \vdots \\ w_{k_2}^2 & -2mw_{k_2}^4 \end{bmatrix} \tag{3.38b}$$

$$\{X_2\} = \begin{Bmatrix} Q_{k_1} - m^2(w_m^2 - w_{k_1}^2)^2 \\ Q_{k_1+1} - m^2(w_m^2 - w_{k_1+1}^2)^2 \\ \vdots \\ Q_{k_2} - m^2(w_m^2 - w_{k_2}^2)^2 \end{Bmatrix} \tag{3.38c}$$

$$\{\varepsilon\} = (\varepsilon_{k_1} \quad \varepsilon_{k_1+1} \quad \cdots \quad \varepsilon_{k_2})^T. \tag{3.38d}$$

Note that here, as in the identification of the parameters of the second-order system, only a portion of the Equations 3.37 will be

used in the parameter identification. In particular, the identification is performed in the frequency range (w_{k_1}, w_{k_2}). This frequency range can be chosen as before, using the guidelines presented following Equation 3.29. In terms of these matrices, Equations 3.37 can be expressed

$$[X_1]\{b\} - \{X_2\} = \{\varepsilon\} \tag{3.39}$$

We wish to find the vector $\{b\}$ which minimizes the constant $\varepsilon^2 = \{\varepsilon\}^T\{\varepsilon\}$. It can be shown (see, for example, Reference 6) that this is

$$\{b\} = ([X_1]^T[X_1])^{-1}\,[X_1]^T\{X_2\} \tag{3.40}$$

When b_1 and b_2 have been computed, a_1 and a_2 can be found from

$$a_1 = \sqrt{b_1}, \quad a_2 = b_2/a_1 \tag{3.41}$$

The constants a_0, a_1, and a_2, defined in Equations 3.33 and 3.41, are the parameters of the third-order linear system, Equation 3.4, whose response best matches the hysteretic response $\ddot{z}(t)$, defined earlier in this section.

Some numerical examples are presented in Section 5. These demonstrate the use of all the parameter identification techniques outlined above. Moreover, the examples compare the energy dissipated by the equivalent systems of Equation 3.4 to the energy dissipated in some actual nonlinear systems.

4.0 Error Analysis

In the previous section, two techniques used to establish the model parameters for hysteretic systems were presented. Both time domain and frequency domain approaches for parameter estimation were outlined. At various points in Section 3, allusions to the potential for presence of noise in the measured input and

output signals were made. The approaches chosen for use in parameter identification were chosen for their capacity to accurately estimate system parameters in the presence of noise.

In this section we show how an approximate analysis of the accuracy of the estimated parameters can be executed, when the parameters are estimated using the frequency domain approach. The presence of noise in the measured inputs and outputs affects this accuracy.

In this analysis, the following assumptions are made. 1) There exists in nature a true input, f(t), and a true structural response, $\ddot{z}(t)$. These functions possess exact derivatives and integrals, and if these were known, then any of the parameter identification techniques given in Section 3 could be used to establish the parameters in the model, Equation 3.4, exactly. 2) The measured structural input and response may contain a noise component, in practice. When noise is present in a measured input or response, it appears as an additive term. When noise is present in the measured input or response, it is zero-mean, normally-distributed, band-limited white noise. Noise signals added to the input and output are independent. When the structural input and output signals are discretized at a time interval of Δt, the cutoff frequency for the noise signals is $1/2\Delta t$ hertz.

In the error analysis to follow, we will explicitly consider the effects of measurement noise on parameter identification. The effects of nonlinearity of the measured system response, and accuracy of the Fourier transform will not be considered.

Recall from Section 3 that when the frequency domain approach is used to estimate the parameters a_j, j=0, ... M+1, these parameters may be estimated using a two-step procedure. In the first step, a_0 is estimated, and then the remaining parameters, a_j, j=1, ... M+1, are estimated. a_0 is estimated by

noting the minimum value in $Q_k + \varepsilon_k$, k=0, ... n/2, where Q_k is defined

$$Q_k = \frac{|F_k|^2}{|Z_k|^2}, \qquad k=0, \ldots n/2 \tag{4.1}$$

We now consider the effect that the presence of noise on the input and output have on Q_k.

In Section 3 it was stated that the input forcing function f_ℓ, ℓ=0, ... n-1 and the response acceleration, $\ddot{z}_\ell$, ℓ=0, ... n-1 are assumed known. When the measured forcing function and response include noise, these functions become $f_\ell + n_\ell$, ℓ=0, ... n-1, and $\ddot{z}_\ell + s_\ell$, ℓ=0, ... n-1, respectively. n_ℓ and s_ℓ, ℓ=0, ... n-1, are the input and response noise random processes. These are, as stated above, zero-mean, normally-distributed, white noise, random processes. These are discrete time random processes. The white noise assumption implies that all random variable n_ℓ, n_r are independent for $\ell \neq r$; s_ℓ and s_r are independent for $\ell \neq r$. The random processes n_ℓ, ℓ=0, ... n-1, is independent of s_ℓ, ℓ=0, ... n-1. The variances of the random processes n_ℓ and s_ℓ, ℓ=0, ... n-1 will be denoted σ_n^2 and σ_s^2, respectively.

Since n_ℓ and s_ℓ, ℓ=0, ... n-1 are normally-distributed, random processes, they are fully characterized by their first- and second-order moments. The mathematical expressions which summarize the assumptions listed above follow. The zero mean assumption is expressed

$$E[n_\ell] = E[s_\ell] = 0, \qquad \ell=0, \ldots n-1 \tag{4.2}$$

where $E[\cdot]$ refers to the operation of expectation. The autocorrelation functions of the random processes n_ℓ and s_ℓ, ℓ=0, ... n-1 reflect the white noise assumption. These are

$$E[n_\ell n_r] = \sigma_n^2 \delta_{\ell r}, \quad \ell, r=0, \ldots n-1 \tag{4.3a}$$

$$E[s_\ell s_r] = \sigma_s^2 \delta_{\ell r}, \quad \ell, r=0, \ldots n-1 \tag{4.3b}$$

where $\delta_{\ell r}$ is the Kronecker delta.

To execute a frequency domain analysis, we must find the discrete Fourier transforms (DFT) of $f_\ell + n_\ell$ and $\ddot{z}_\ell + s_\ell$, $\ell=0, \ldots n-1$. The DFTs of f_ℓ and $\ddot{z}_\ell$, $\ell=0, \ldots n-1$, have been expressed F_k and $-w^2 Z_k$, $k=0, \ldots n/2$, respectively. The DFTs of n_ℓ and s_ℓ, $\ell=0, \ldots n-1$, are defined

$$N_k = \Delta t \sum_{\ell=0}^{n-1} n_\ell \, e^{-i2\pi\ell k/n}, \quad k=0, \ldots n/2 \tag{4.4a}$$

$$S_k = \Delta t \sum_{\ell=0}^{n-1} s_\ell \, e^{-i2\pi\ell k/n}, \quad k=0, \ldots n/2 \tag{4.4b}$$

The sequences N_k and S_k, $k=0, \ldots n/2$, form normally distributed random processes since each of the values N_k and S_k, is a linear function of a sequence of normally-distributed random variables. In view of this, N_k and S_k, $k=0, \ldots n/2$, can be fully characterized in terms of their first- and second-order moments. Those are listed below.

Each of the random variables, N_k, S_k, is a complex quantity, and possesses a real and an imaginary part. In terms of these, N_k and S_k can be expressed

$$N_k = N_{Rk} + i\, N_{Ik} \qquad k=0, \ldots n/2 \tag{4.5a}$$

$$S_k = S_{Rk} + i\, S_{Ik} \qquad k=0, \ldots n/2 \tag{4.5b}$$

Since the underlying random processes, n_ℓ, s_ℓ, $\ell=0, \ldots n-1$, have zero mean, and since the DFTs are linear functions of these, the DFTs have a zero mean.

$$E[N_{Rk}] = E[N_{Ik}] = 0 \tag{4.6a}$$

$$E[S_{Rk}] = E[S_{Ik}] = 0 \tag{4.6b}$$

The correlation functions for N_{Rk} and N_{Ik} can be generated from the formulas

$$E[N_k\ N_r] = \Delta t^2 \sum_{\ell=0}^{n-1}\sum_{s=0}^{n-1} E[n_\ell\ n_s]\ e^{-i2\pi(k\ell + rs)/n}$$

$$= \begin{cases} n\sigma_n^2\ \Delta t^2 & k = r = 0 \\ 0 & \text{otherwise} \end{cases} \tag{4.7a}$$

$$E[N_k\ N_r^*] = \Delta t^2 \sum_{\ell=0}^{n-1}\sum_{s=0}^{n-1} E[n_\ell\ n_s]\ e^{-i2\pi(k\ell - rs)/n}$$

$$= \begin{cases} n\sigma_n^2\ \Delta t^2 & k = r \\ 0 & k \neq r \end{cases} \tag{4.7b}$$

Using Equation 4.5a, we can form $E[N_k\ N_r]$ and $E[N_k\ N_r^*]$. The results can be equated to Equations 4.7a and b. This yields

$$E[N_{Rk}\ N_{Rr}] = \begin{cases} n\sigma_n^2\ \Delta t^2/2 & k = \ell \neq 0 \\ n\sigma_n^2\ \Delta t^2 & k = \ell = 0 \\ 0 & k \neq \ell \end{cases} \tag{4.8a}$$

$$E[N_{Ik}\ N_{Ir}] = \begin{cases} n\sigma_n^2\ \Delta t^2/2 & k = \ell \neq 0 \\ 0 & k = \ell = 0 \\ 0 & k \neq \ell \end{cases} \qquad (4.8b)$$

$$E[N_{Rk}\ N_{Ir}] = 0 \qquad \text{all } k, \ell \qquad (4.8c)$$

Similarly, we can show

$$E[S_{Rk}\ S_{Rr}] = \begin{cases} n\sigma_s^2\ \Delta t^2/2 & k = \ell \neq 0 \\ n\sigma_s^2\ \Delta t^2 & k = \ell = 0 \\ 0 & k \neq \ell \end{cases} \qquad (4.9a)$$

$$E[S_{Ik}\ S_{Ir}] = \begin{cases} n\sigma_s^2\ \Delta t^2/2 & k = \ell \neq 0 \\ 0 & k = \ell = 0 \\ 0 & k \neq \ell \end{cases} \qquad (4.9b)$$

$$E[S_{Rk}\ S_{Ir}] = 0 \qquad \text{all } k, \ell \qquad (4.9c)$$

These moments completely summarize the random processes N_k and S_k, k=0, ... n/2. Apparently, the underlying random processes N_{Rk}, N_{Ik}, S_{Rk} and S_{Ik}, k=0, ... n/2, are mutually-independent, zero-mean, normally-distributed, and nearly band-limited white noise.

When noise is present in the input and response readings, Equation 4.1 cannot be established since the noise-free values of F_k and Z_k, k=0, ... n/2, will not be known. Rather, input and response functions including noise will be used to form the ratio, and Equation 4.1 will be replaced by

$$Q'_k = \frac{|F_k + N_k|^2}{\left|Z_k - (S_k/w_k^2)\right|^2}, \quad k=0, \ldots n/2. \tag{4.10}$$

(The $-w^2$ term is included in the denominator since $\ddot{z}_\ell + s_\ell$, $\ell=0, \ldots n-1$, is measured and its DFT is $-w_k^2 Z_k + S_k$, $k=0, \ldots n/2$.) We wish to know the *minimum* value in $|F_k|^2/|Z_k|^2$, but when noise is present, we must estimate this using Q'_k. Q'_k is a random variable since it is a function of the random variables, N_k and S_k. Since the parameter a_0 will be estimated using the minimum value of Q'_k, the estimator for a_0 is a random variable. Its probability distribution is a function of the probability distribution of Q'_k. The probability distribution of Q'_k is quite complicated because of the form of its functional dependence on N_k and S_k. However, the moments of Q'_k can be easily estimated. The first step toward accomplishing this task is to compute the moments of the numerator and denominator of Q'_k.

Consider the numerator in Equation 4.10. Its mean and variance can be found using the Expressions 4.8. Note that F_k has been assumed a nonrandom (though unknown) constant. The mean of $|F_k + N_k|^2$ is the expected value of $F_k + N_k$ times its complex conjugate. This is

$$E[|F_k + N_k|^2] = |F_k|^2 + n\sigma_n^2 \Delta t^2, \quad k=0, \ldots n/2. \tag{4.11a}$$

The variance of $|F_k + N_k|^2$ is the mean square of $|F_k + N_k|^2$ minus the square of the mean. This is

$$V[|F_k + N_k|^2] = n^2\sigma_n^4 \Delta t^4 + 2n\sigma_n^2 \Delta t^2 |F_k|^2 + 2\delta_{ko} n\sigma_n^2 \Delta t^2(F_{RO}^2 + F_{IO}^2), \quad k=0, \ldots n/2 \tag{4.11b}$$

where δ_{ko} is the Kronecker delta. The mean and variance of the denominator of Equation 4.10 can also be found and these are

$$E[|Z_k - S_k/w_k^2|^2] = |Z_k|^2 + n\sigma_s^2 \Delta t^2/w_k^4, \quad k=0, \ldots n/2 \qquad (4.12a)$$

$$V[|Z_k - S_k/w_k^2|^2] = n^2\sigma_s{}^4\Delta t^4/w_k^8 + 2n\sigma_w^2\Delta t^2|Z_k|^2/w_k^4 + 2\,\delta_{ko}\, n\sigma_s{}^2\Delta t^2(Z_{RO}^2 + Z_{IO}^2)/w_k^4, \quad k=0, \ldots n/2 \qquad (4.12b)$$

So far, the moments established in Equations 4.11 and 4.12 are exact, given the assumptions concerning n_ℓ and s_ℓ, $\ell=0, \ldots n-1$, listed previously. We now form approximations for the moments of Q_k' in Equation 4.10.

Recall that if X and Y are independent random variables and if Z is defined as the ratio of these, then the first two moments of Z can be approximated. Let

$$Z = X/Y. \qquad (a)$$

Then

$$E[Z] \tilde{=} E[X]/E[Y] \qquad (b)$$

$$V[Z] \tilde{=} ((E[X])^2\, V[Y] + (E[Y])^2\, V[X])/(E[Y])^4. \qquad (c)$$

Based on these formulas, the approximate values for the mean and variance of Q_k' can be written

$$E[Q_k'] \tilde{=} E[|F_k + N_k|^2]\Big/E[|Z_k - S_k/w_k^2|^2], \quad k=0,1, \ldots n/2 \qquad (4.13a)$$

and

$$V[Q_k'] = \frac{\{E[|F_k+N_k|^2]\}^2 V[|F_k+N_k|^2]+\{E[|Z_k-S_k/w_k^2|^2]\}^2 V[|Z_k-S_k/w_k^2|^2]}{\{E[|Z_k-S_k/w_k^2|^2]\}^4}$$

$$k=0, \ldots n/2. \qquad (4.13b)$$

These moments characterize the distribution of Q_k', k=0, ... n/2, but do not completely define it. As mentioned above, the distribution of Q_k' is quite complicated. For the purposes of this approximate analysis, however, we can assume that Q_k' has a distribution which takes a relatively simple, common form. We assume Q_k' to be normally distributed. Then the distribution of Q_k' is fully described by $E[Q_k']$ and $V[Q_k']$. With this assumption, the analysis can proceed.

The estimated value of the parameter a_0 depends on the minimum value of Q_k', k=0, ... n/2. Let Ω_m be the frequency where Q_k' assumes its minimum. Then we can write

$$\begin{aligned} P(\Omega_m = w_k) &= P(Q_k' \text{ is the smallest of the values } Q_j', \ j=0, \ldots n/2) \\ &= P\Big(\bigcap_{j\neq k} Q_k' \leq Q_j'\Big) \\ &= P\Big(\bigcap_{j\neq k} Q_k' - Q_j' \leq 0\Big) \qquad k=0, \ldots n/2 \end{aligned} \qquad (4.14)$$

Here $\bigcap_{j\neq k} Q_k' \leq Q_j'$ simply refers to the joint event where Q_k' is equal to or less than each Q_j', $j\neq k$. The last step simply rearranges the inequality. Equations 4.8 and 4.9 show that the random variables Q_k' and Q_j' are independent when $j\neq k$. Therefore, Equation 4.14 can be written

$$P(\Omega_m = w_k) = \overline{\prod_{j\neq k}} P(Q_k' - Q_j' \leq 0)$$

$$= \overline{\prod_{j\neq k}} F_{Q_k' - Q_j'}(0) \qquad k=0, \ldots n/2 \tag{4.15}$$

where $F_{Q_k' - Q_j'}(x)$ is the cumulative distribution function of $Q_k' - Q_j'$. (Since Q_k' is assumed normally distributed, then $Q_k' - Q_j'$ will also be normally distributed.)

Finally, Equation 3.27 in Section 3 establishes the formula for a_0 as

$$a_0 = mw_m^2. \tag{4.16}$$

In terms of this formula, the probability distribution for the estimator of a_0 is

$$P(A_0 = \alpha) = \begin{cases} P(\Omega_m = \sqrt{\alpha/m}) \ , \ \alpha = mw_k^2, \ k=0, \ldots n/2 \\ 0 \qquad\qquad\qquad \text{otherwise} \end{cases} \tag{4.17}$$

where A_0 is defined as the random variable used to estimate a_0. This formula provides an approximate probabilistic description of

the character of the estimator A_0. We expect that when the function Q'_k, k=0, ... n/2, has a pronounced trough near its minimum, the probability distribution of A_0 will be tightly concentrated around mw_m^2. When Q'_k, k=0, ... n/2, is relatively shallow, the distribution of A_0 may show considerable spread.

In order to establish confidence intervals on the underlying value of a_0, a probability relation between the underlying value and its estimator, A_0, must be established. This relation can be solved for a_0 to establish confidence intervals on a_0. For the approximate purposes of this analysis, we simply assume that A_0 is a normally-distributed random variable with mean a_0. (The assumption that A_0 has mean a_0 is not exactly correct, as may be noted from Equation 3.26.) Then confidence intervals on the underlying constant, a_0, can be written

$$C(mw_m^2 - b\,\hat{\sigma}_a \leq a_0 \leq mw_m^2 + b\,\hat{\sigma}_a) = 2\Phi(b) - 1 \qquad b > 0 \tag{4.18}$$

where $\hat{\sigma}_a^2$ is the estimated variance of A_0 obtained using Equation 4.17, $\Phi(\cdot)$ is the standard, normal cumulative distribution function; and b is a constant related to the confidence level of the established intervals. This concludes the error analysis on the parameter a_0. The error analysis on a_j, j=1, ... M+1, can now be performed.

Error analysis on the variable a_1 will be performed for the case where M=0. This analysis will be conditioned on our knowledge of the value (or estimate) of a_0. This approach is taken since Equations 3.28, 3.29, and 3.34 through 3.40 rely on this knowledge of a_0. When noise is present in the structural input and response measurements, the formula used to estimate a_1 becomes

$$A_1^2 = \left(\sum_k w_k^4\right)^{-1} \left\{\sum_k Q_k' w_k^2 - \sum_k m(w_m^2 - w_k^2)^2 w_k^2\right\}$$

(4.19)

The random variable Q_k' has replaced Q_k in Equation 3.29; therefore, A_1^2 is the random variable estimator for the underlying parameter a_1^2. The mean and variance of A_1^2, conditioned on a_0, can be established based on the mean and variance of Q_k' given in Equations 4.13. These are

$$E[A_1^2|a_0] = \left(\sum_k w_k^4\right)^{-1} \left\{\sum_k E[Q_k'] w_k^2 - \sum_k m(w_m^2 - w_k^2)^2 w_k^2\right\}$$

(4.20a)

$$V[A_1^2|a_0] = \left(\sum_k w_k^4\right)^{-2} \left\{\sum_k V[Q_k'] w_k^4\right\} \qquad (4.20b)$$

With this information, an approximate conditional probability distribution for A_1^2 given a_0 can be established. We take the conditional distribution of A_0^2 to be normal with the mean and variance listed above. Using these assumptions, the confidence intervals on a_1^2 can be written

$$C\left(E[A_1^2|a_0] - b\sqrt{V[A_1^2|a_0]} \leq a_1^2 < E[A_1^2|a_0] + b\sqrt{V[A_1^2|a_0]} \;\middle|\; a_0\right)$$
$$= 2\Phi(b) - 1 \qquad b > 0$$

(4.21)

For various values of b, and using the estimated moments of Equations 4.20, Equation 4.21 sets the confidence limits for a_1^2.

We now perform an error analysis on the variables a_1 and a_2 for the case where M=1. As above, we condition our analysis on knowledge of the value of a_0. Equation 3.40 establishes an expression for the two-dimensional vector $\{b\}$. Its elements, b_1 and b_2, are simply related to a_1 and a_2, so we concentrate our preliminary analysis on $\{b\}$. When the value of a_0 is specified, the matrix $[X_1]$ in Equation 3.40 is known. When Q_k' replaces Q_k in Equation 3.38c, $\{b\}$ must be replaced by a random vector. We perform the specified replacement to obtain

$$\{B\} = [R]\ \{X_2'\} \tag{4.22}$$

where $\{B\}$ is the estimator random vector for $\{b\}$, $\{X_2'\}$ is the vector whose form is Equation 3.38c with Q_k replaced by Q_k', and

$$[R] = \left([X_1]^T\ [X_1]\right)^{-1}\ [X_1]^T \tag{4.22a}$$

where $[X_1]$ is defined in Equation 3.38b. The conditioned mean value of $\{B\}$ is

$$E[\{B\} \mid a_0] = [R]\ E\{X_2'\} \tag{4.23}$$

where

$$E\{X_2'\} = \begin{Bmatrix} E[Q_{k_1}'] - m^2(w_m^2 - w_{k_1}^2)^2 \\ E[Q_{k_1+1}'] - m^2(w_m^2 - w_{k_1+1}^2)^2 \\ \vdots \\ E[Q_{k_2}'] - m^2(w_m^2 - w_{k_2}^2)^2 \end{Bmatrix} \tag{4.23a}$$

The expression for $E[Q_k']$ is given in Equation 4.13a. Equation 4.23 provides the mean value of B_1 and B_2, given a_0.

The conditioned covariance matrix for $\{B\}$ is obtained using the following procedure: 1) Find the mean value of the product $\{B\}\{B\}^T$. This is done using Equations 4.22, 3.38c and 4.13, and by noting that Q'_k and Q'_j are independent for $k \neq j$. 2) Subtract from this the product $E[\{B\} | a_0] (E[\{B\} | a_0])^T$. The result is

$$[K_{BB|a_0}] = [R][K][R]^T \tag{4.24}$$

where the diagonal elements of [K] are the variances of the random variables Q'_k, $k=k_1, \ldots k_2$, and the off-diagonal terms are zero.

$$[K] = \begin{bmatrix} V[Q'_{k_1}] & 0 & \cdots & 0 \\ 0 & V[Q'_{k_1+1}] & \cdots & 0 \\ \vdots & \vdots & & \vdots \\ 0 & 0 & & V[Q'_{k_2}] \end{bmatrix} \tag{4.24a}$$

The diagonal elements in $[K_{BB|a_0}]$ are the variances of B_1 and B_2, given a_0. Equations 4.23 and 4.24 define the first- and second-order moments of $\{B\}$. These can be used to establish the moments for the estimators of a_1 and a_2.

Let A_j be the random variable of the estimator a_j, $j=1,2$. Then, according to Equation 3.41, we can write

$$A_1^2 = B_1, \quad A_2^2 = B_2^2/B_1 \tag{4.25}$$

The conditional moments of A_1^2 can be obtained by directly taking the mean and variance on both sides of the first of Equations 4.25.

$$E[A_1^2 \mid a_0] = E[B_1 \mid a_0] \tag{4.26a}$$

$$V[A_1^2 \mid a_0] = V[B_1 \mid a_0] \tag{4.26b}$$

The moments on the right-hand side are defined in Equations 4.23 and 4.24. The moments of A_2^2 must be approximated since the expression for A_2^2 involves a ratio and a power of B_1 and B_2. Using Equations a, b and c, listed previously in this section, we can show that the conditional moments of A_2^2 are approximately

$$E[A_2^2 \mid a_0] \tilde{=} E[B_2^2 \mid a_0]/E[B_1 \mid a_0] \tag{4.27a}$$

$$V[A_2^2 \mid a_0] \tilde{=} \frac{(E[B_2^2 \mid a_0])^2 V[B_1 \mid a_0] + (E[B_1 \mid a_0])^2 V(B_2^2 \mid a_0)}{(E[B_1 \mid a_0])^4} \tag{4.27b}$$

where

$$E[B_2^2 \mid a_0] = V[B_2 \mid a_0] + (E[B_2 \mid a_0])^2 \tag{4.27c}$$

$$V[B_2^2 \mid a_0] = 3(V[B_2 \mid a_0])^2 \tag{4.27d}$$

The moments in Equations 4.27c and 4.27d can be obtained directly from Equations 4.23 and 4.24. These can be used to establish Equations 4.27a and 4.27b. Equation 4.27d uses the normal approximation to estimate the variance of B_2^2.

When we establish the relation between each underlying parameter, a_j, and its estimator random variable, A_j, $j=1,2$, and when we find the probability distribution of the A_j, $j=1,2$,

we can write confidence intervals on the a_j. For the approximate purposes of the present analysis, we simply assume that the A_j^2, j=1,2, are normally-distributed random variables. Then the confidence intervals on the a_j, j=1,2, can be written

$$C(E[A_j^2 \mid a_0] - c\sqrt{V[A_2^2 \mid a_0]} \leq a_j^2 < E[A_j^2 \mid a_0] + c\sqrt{V[A_2 \mid a_0]})$$
$$= 2\Phi(c) - 1, \; j=1,2, \; c > 0 \qquad (4.28)$$

This formula reflects our confidence that a_j^2 falls within $\pm c\sqrt{V[A_2^2 \mid a_0]}$ of its estimated value.

Equations 4.18, 4.21, and 4.28 establish confidence intervals on the parameters a_j, j=0,1,2. The confidence intervals on a_1 and a_2 are actually conditioned on the value of a_0. These could be made unconditional by deriving them from the joint probability distribution for A_0, A_1, and A_2. This joint distribution could be obtained by multiplying the conditional distribution of A_1 and A_2 by the distribution of A_0. But this was not done in the present analysis for the following reason. The separation of the error analysis into two sequential parts follows the approach used in the parameter identification of Section 3. First, the value of a_0 is estimated. Then this value is used in the identification procedure to find a_1 and a_2.

Simplifying and approximating assumptions regarding the distributions of the parameter estimators, A_0, A_1, and A_2, have been made freely throughout this analysis. These assumptions certainly affect the accuracy of this error analysis, but we feel that useful results can still be obtained using the formulas presented here. In particular, when the variance of the noise on the measured structural input and response are small, we expect that the analyses of this section will be accurate.

The error analysis for the time domain approaches to parameter identification are not included in this report for two reasons. 1) The time domain analyses developed in this report yield

results which are more sensitive to the presence of noise than the frequency domain approaches. Therefore, these approaches will be less useful to us in practice. 2) The time domain error analyses are quite difficult to implement in a practical computation scheme.

5.0 Numerical Examples

In this section, numerical examples are presented which demonstrate the use of the analytic procedures developed in the previous sections. Two examples demonstrating the time domain approach to parameter identification are summarized. One example showing the frequency domain approach is presented. The examples demonstrate the identification of the model parameters for linear and hysteretic, single-degree-of-freedom (SDF) structures, both when measurement noise is and is not present.

The input used to excite the SDF systems in all the numerical examples is a decaying exponential, oscillatory function. It is generated using the formula

$$f(t) = e^{-\alpha t} \left[\sum_{j=1}^{N} c_j \cos(w_j t - \phi_j)\right], \quad 0 \leq t \leq T. \qquad (5.1)$$

α, c_j, j=1, ... N, and w_j, j=1, ... N, are constants. ϕ_j, j=1, ... N, are phase angles which are random variable realizations; the underlying random variables are independent and uniformly distributed on the interval $(0, 2\pi)$. α is the input decay rate. The c_j, j=1, ... N, are constants determining the amplitudes of input components. In all cases described below, all the values of the c_j are taken as equal to c. w_j, j=1, ... N, are the frequencies where the input components are generated. In all examples shown here, the w_j, j=1, ... N, are equally spaced in an interval including the characteristic frequency of the system being analyzed. The forcing function defined above was generated

at discrete times for use in the numerical examples. Specifically, f(t) was evaluated at the times $t = t_\ell = \ell\Delta t$, $\ell=0, \ldots n-1$. A computer program, named FORCE, which generates the inputs of Equation 5.1 was used in these numerical examples.

It was necessary to compute both linear and hysteretic, SDF structure responses in the examples. This was done using an incremental equations approach, described, for example, in Reference 8. A computer program, named BILIN, was written to execute the structural response computations. BILIN can be used to find the displacement, velocity, and acceleration response of a bilinear hysteretic structure to an arbitrary input. It also computes the energy dissipated by the structure during its response.

Two basic approaches for solving the parameter identification problem were proposed in this study. These are the time domain and frequency domain approaches. Two computer programs were written to execute the parameter identifications. These are named TIMEID and FREQID. TIMEID performs time domain parameter identification. It accepts an input signal from FORCE and a computed response from BILIN and then does one of two things. It either submits the data for an immediate parameter identification, or it adds white noise to the input and/or output, and then submits the data for parameter identification. The program can perform the parameter identification directly using Equations 3.4 through 3.12, or it can perform the identification using the integrated equations approach, Equations 3.13 through 3.18. The program can identify the parameters of the second-order model (M=0) or the third-order model (M=1) of Equation 3.4.

The computer program FREQID performs frequency domain parameter identification. It accepts an input signal from FORCE and a computed response from BILIN. If desired, FREQID next adds white noise signals to the input and/or response. Then it performs the

necessary Fourier transforms and other data operations. Following this, the parameter identification is executed. Equations 3.19 through 3.41 are used. The program can identify the parameters of the second-order model (M=0) or the third-order model (M=1) of Equation 3.4.

Once the parameters of Equation 3.4 have been estimated, the energy dissipated by the model is computed; and this is compared to the energy dissipated by the actual system, as computed in BILIN. This computation is the one discussed in Section 2 and given by Equation 2.5b. The energy computations are performed in programs ENED10, for second-order systems, and ENED13, for third-order systems. The computations are performed using an incremental form of the governing Equation 3.4.

The notations for the parameters used in specifying the numerical examples are those used in the text. Some additional notations are defined here. c is the viscous damping in an SDF system. k is the initial stiffness in a bilinear hysteretic structure. k_y is the yield stiffness of a bilinear hysteretic structure. z_y is the yield displacement of a bilinear hysteretic structure. z_{max} is the maximum displacement of an SDF structure.

In the following numerical examples, four basic problem types are solved. These are summarized below.

(1) An input is generated using Equation 5.1. The input is used to excite a linear SDF system with viscous damping. The structural input and response are stored, and no noise signals are added to the input and response. Then the input and response are used to identify the model parameters, a_j, j=0, ... M+1, from Equation 3.4.

(2) An input is generated as in 1, above, but here the response of a bilinear hysteretic system is computed. No noise signals are added to the input and response. The input and response are used to identify the model parameters, a_j, j=0, ... M+1.

(3) This case is the same as 1, above, but here noise signals are added to the input and response. Then the parameters a_j, j=0, ... M+1 are identified.

(4) This case is the same as 2, above, but here noise signals are added to the input and response. Then the parameters a_j, j=0, ... M+1 are identified.

In all four cases, the parameters of the second-order model, a_0 and a_1 (M=0), and the third-order model, a_0, a_1, and a_2 (M=1), are identified. Moreover, the energy dissipated by the model system with the identified parameters is computed.

5.1 Example 1

This example solves a parameter identification problem using the direct time domain approach, summarized in Equations 3.4 through 3.12. The parameters of the shock input are listed in Table 5.1. A typical forcing function history generated using these parameters is shown in Figure 5.1a. The derivative of the forcing function is shown in Figure 5.1b.

The responses of some SDF systems to the shock input in Figure 5.1a were computed. First, the response of a linear system was computed for analysis in cases 1 and 5. The computed displacement response is plotted versus time in Figure 5.2a. The SDF structure spring restoring force versus displacement is plotted in Figure 5.2b. The very slightly nonlinear response of an SDF structure was computed for analysis in cases 2 and 6, but this response is not shown. A more nonlinear response was computed for analysis in cases 3 and 7. The displacement response versus time is plotted in Figure 5.3a, and the spring restoring force versus displacement is shown in Figure 5.3b. The first figure shows a residual plastic displacement as the response vibrations diminish. The second graph shows the permanent set as lateral displacement of the horizontal axis intercept. Finally, a very nonlinear response was computed for analysis in cases 4

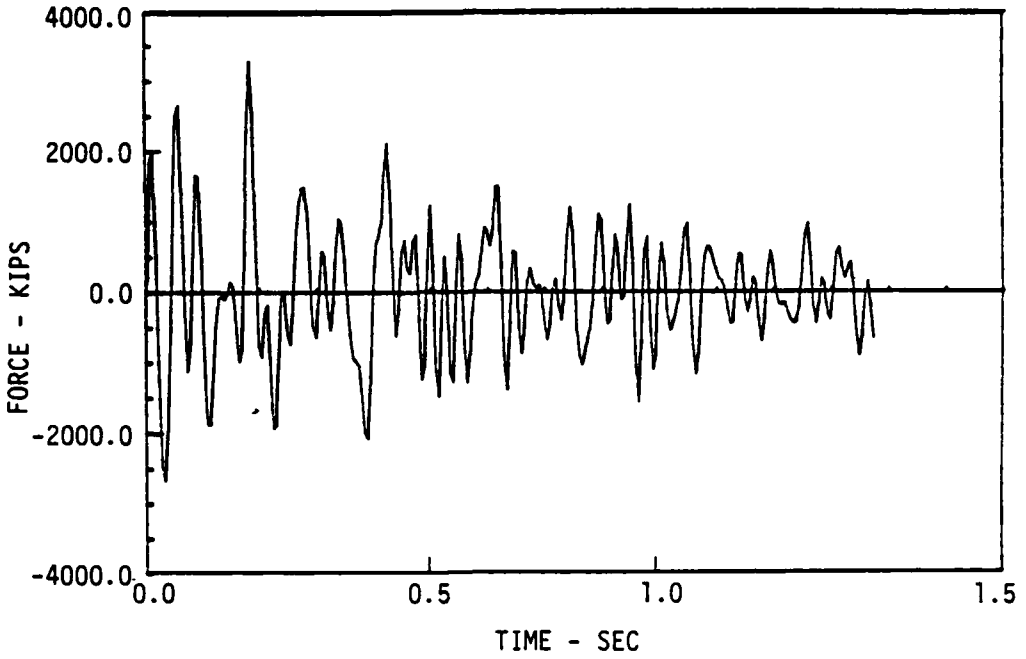

Figure 5.1a. Decaying exponential forcing function for Example 1

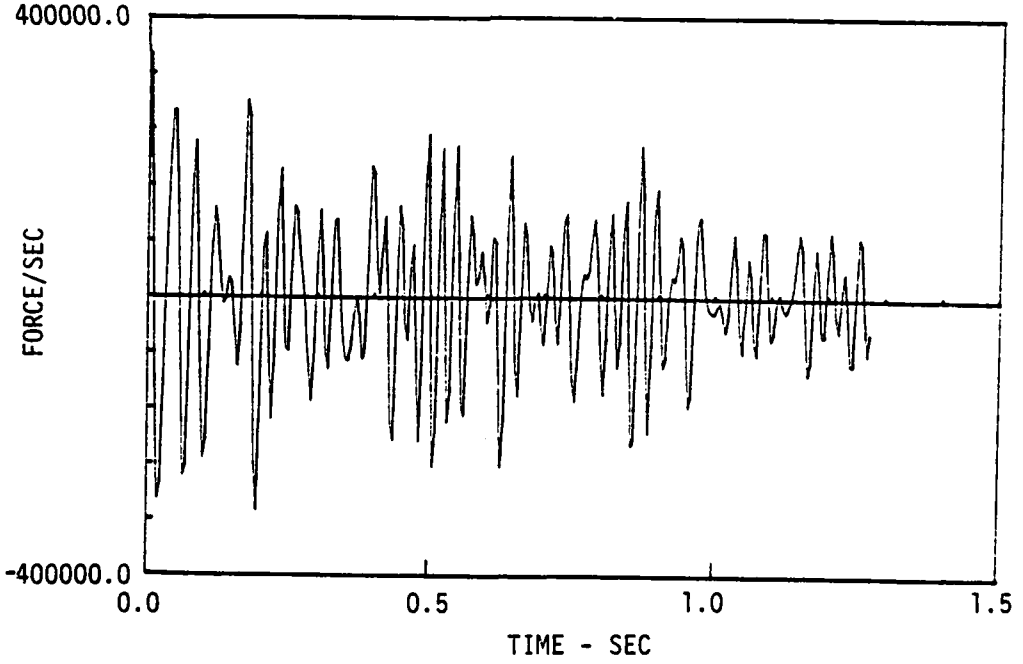

Figure 5.1b. Derivative of forcing function in Figure 5.1a

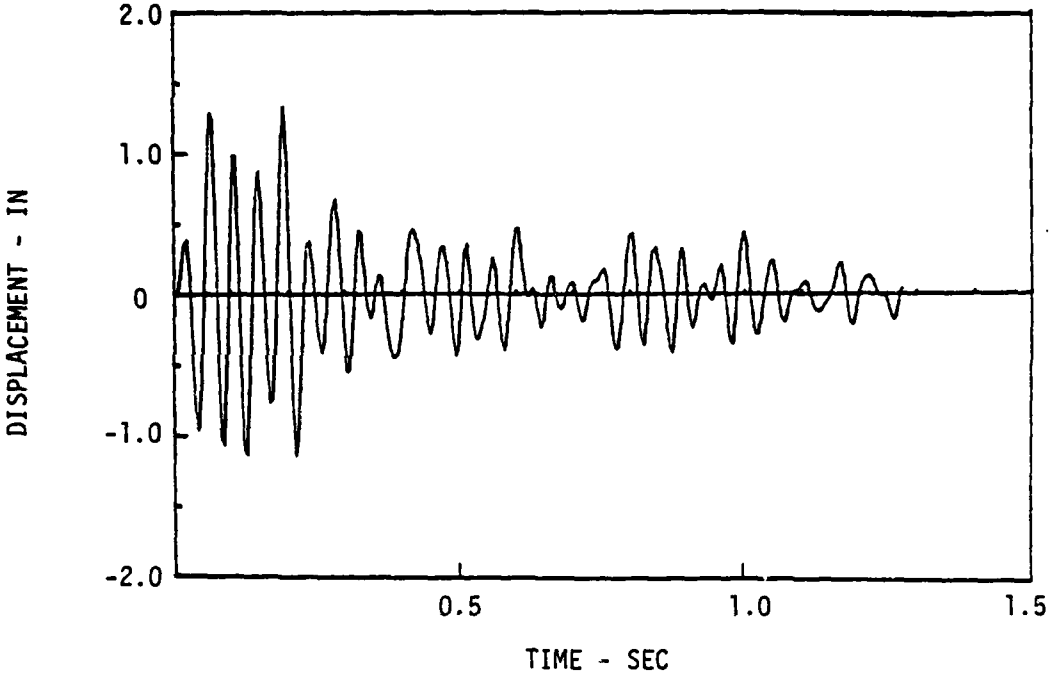

Figure 5.2a. Response of a linear system to the force in Figure 5.1a. $k_y = \infty$

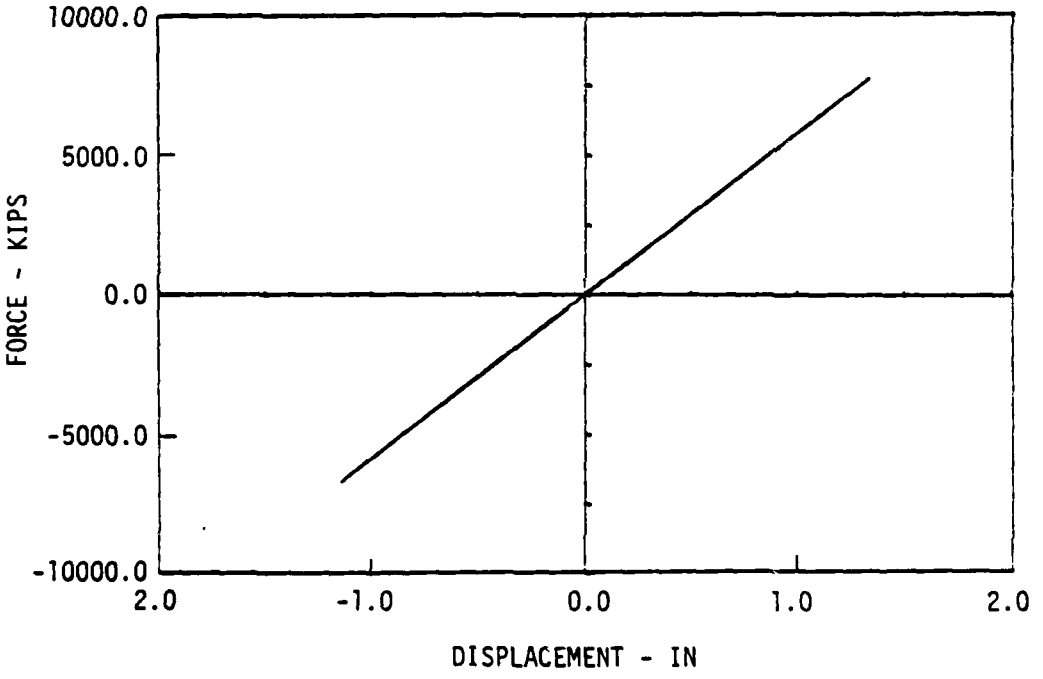

Figure 5.2b. Spring restoring force versus displacement for linear system

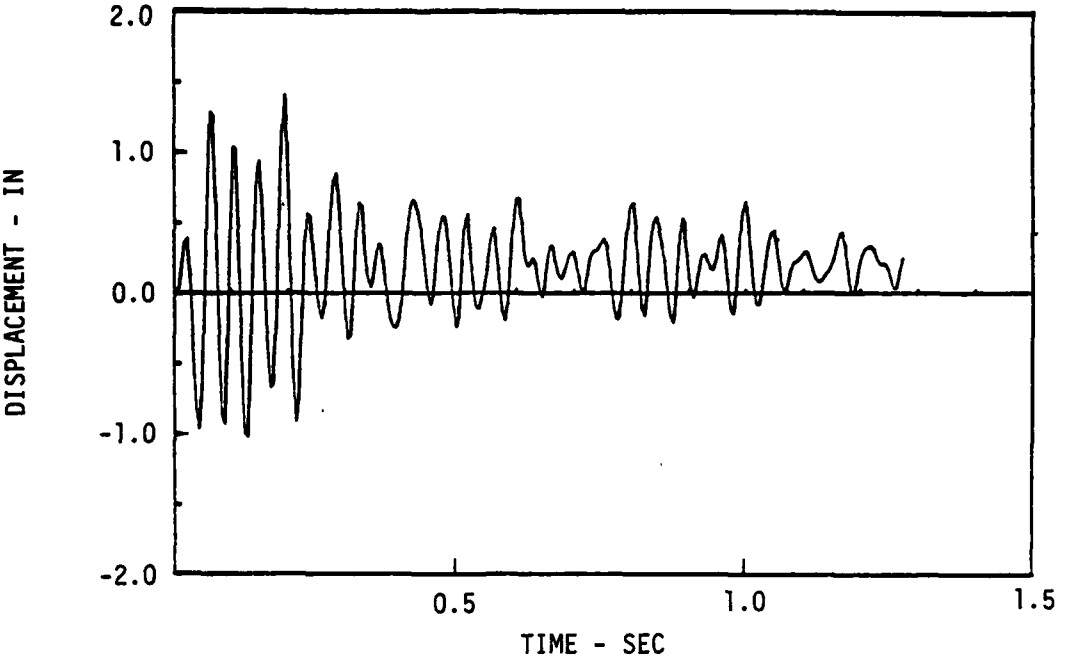

Figure 5.3a. Response of nonlinear system to the force in Figure 5.1a. k_y = 7000

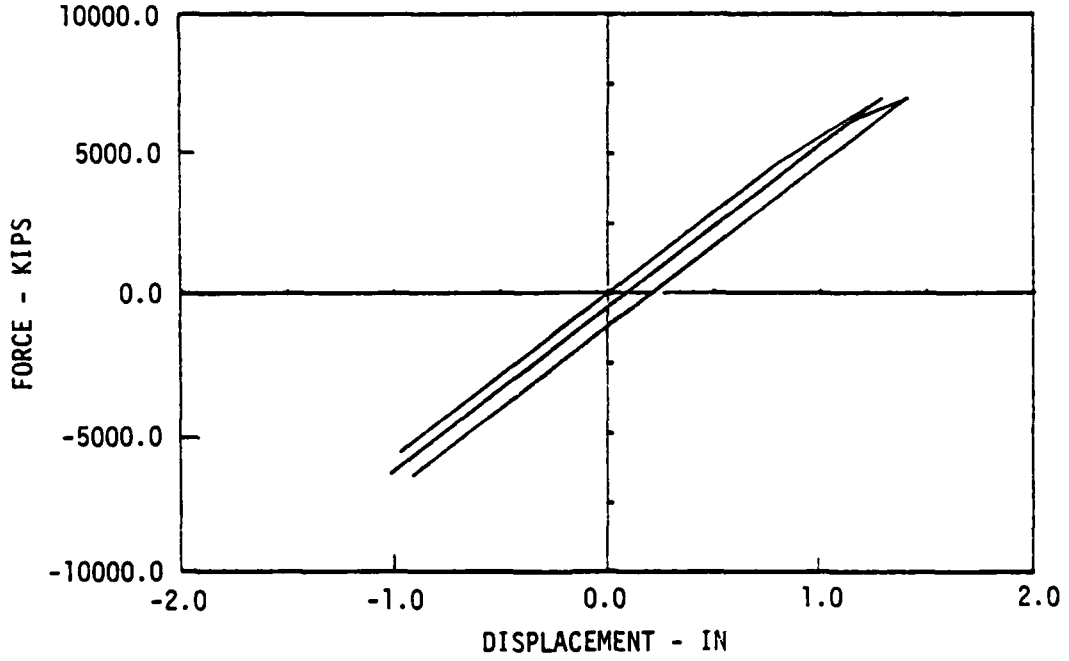

Figure 5.3b. Spring restoring force versus displacement for nonlinear system

Table 5.1. Parameters and Results for Example 1

Input (Structural Excitation)

Case Number	N	α	c	w_1	w_N	n	Δt
1 through 8	50	1.0	300	32.4	1256.4	256	0.005

Structure Parameters

Case Number	m	c	k	k_y	z_y	E_D
1,5	0.259	7.77	5829	-	∞	23292
2,6	0.259	7.77	5829	0	7700	23588
3,7	0.259	7.77	5829	0	7000	23674
4,8	0.259	7.77	5829	0	5000	21959

Identification Parameters and Results

Case Number	M	a_0	a_1	a_2	E_D
1	2	5829	7.77		21533
2	2	5825	7.79		21533
3	2	4574	8.13		21779
4	2	1620	9.69		23844
5	3	5829	7.77	0.0	21533
6	3	5823	7.85	0.0	21498
7	3	2527	99.65	0.0158	20824
8	3	610	108.11	0.0175	18666

and 8. The displacement response versus time is shown in Figure 5.4a and the spring restoring force versus displacement is shown in Figure 5.4b. A considerable permanent set is evident, as the motion diminishes, from the first figure. The second figure shows that large plastic deformations occur in the structure in both directions of motion.

The energy dissipated by each structural system is listed with the structural parameters in Table 5.1. E_D is that energy dissipated due to the action of the inelastic spring and the action of the viscous damper.

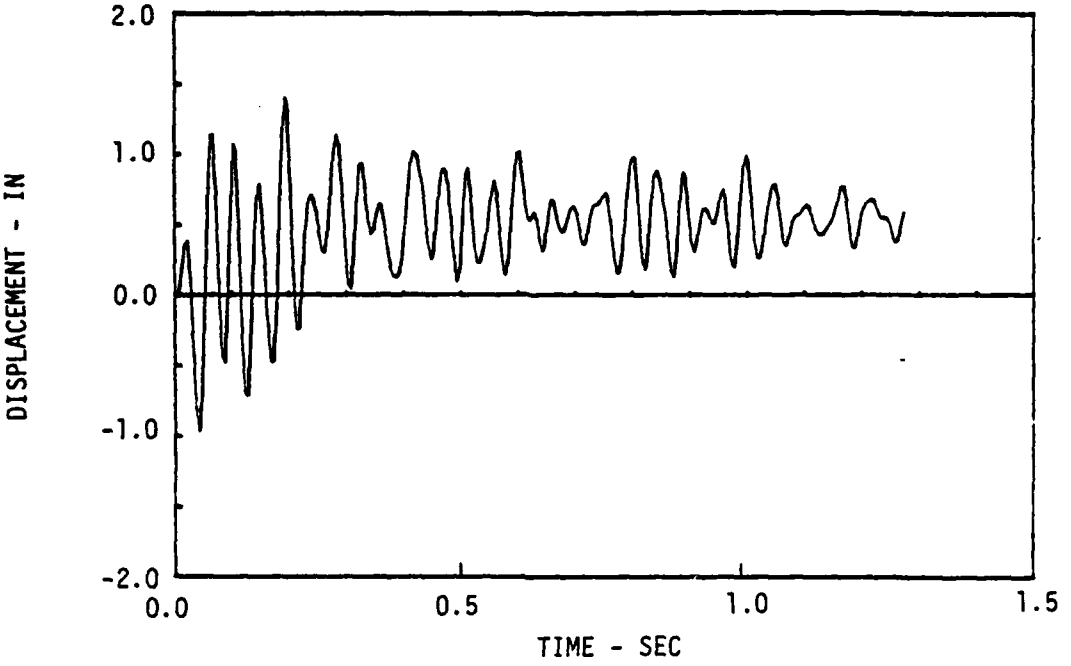

Figure 5.4a. Response of nonlinear system to the force in Figure 5.1a. k_y = 5000

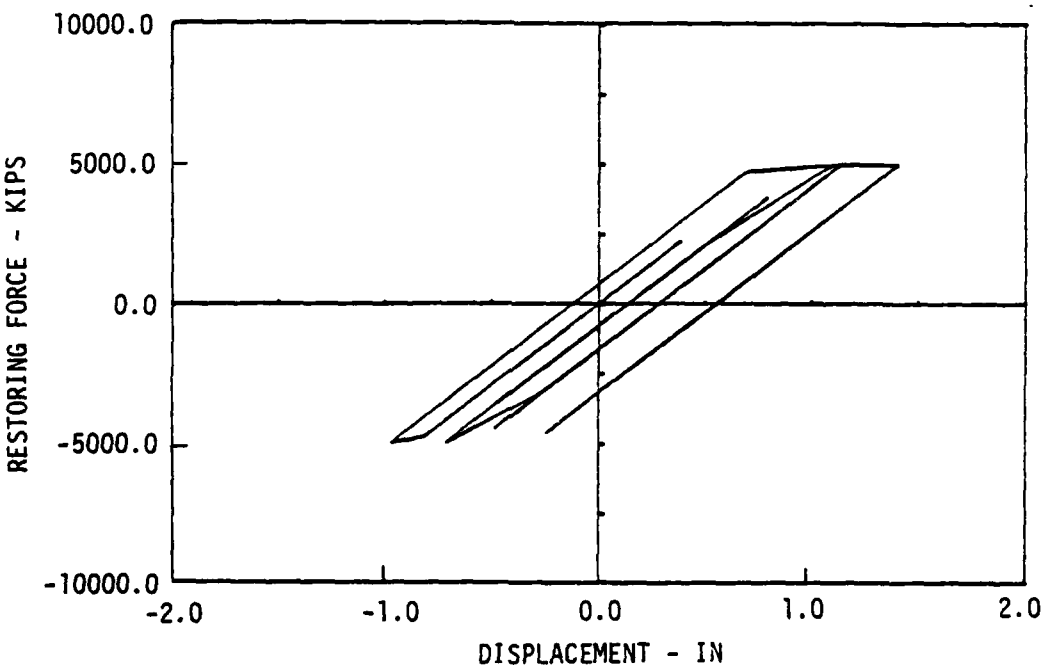

Figure 5.4b. Spring restoring force versus displacement for nonlinear system

Using the forcing function input, described above, and the computed responses, the parameters of the structural systems were identified. The results of the parameter identifications are given in Table 5.1. The energy dissipated when the identified systems respond to the shock input is listed in Table 5.1 next to the identified parameters.

Figures 5.5a through 5.9b show the computed responses of some of the identified systems. The figure titles indicate which systems generate the responses shown. The top (or "a") figures show the computed responses versus time. The bottom (or "b") figures show the computed restoring forces, spring force plus damper force, versus displacements.

Figure 5.10 compares three responses. These are: 1) the actual nonlinear structural response obtained using BILIN in the slightly nonlinear cases 2 and 6, 2) the response executed by the identified model described in case 2, and 3) the response executed by the identified model described in case 6. The two latter responses practically overlay and very nearly equal the actual response.

Figure 5.11a compares the actual nonlinear response of cases 3 and 7 to the second-order (M=0) model response of case 3. Figure 5.11b compares the actual nonlinear response of cases 3 and 7 to the third-order (M=1) model response of case 7. Both models simulate response amplitudes quite well; the third-order model is slightly closer than the second-order model in that the third-order model provides a slightly better phase match to the actual response than the second-order model.

In this numerical example, no cases are included where noise was added to the forcing function input and/or the acceleration response. Such cases were analyzed, but the results were so poor that they are not summarized here. These results showed that the direct, time domain parameter identification technique is not effective in parameter analysis when recording noise is present.

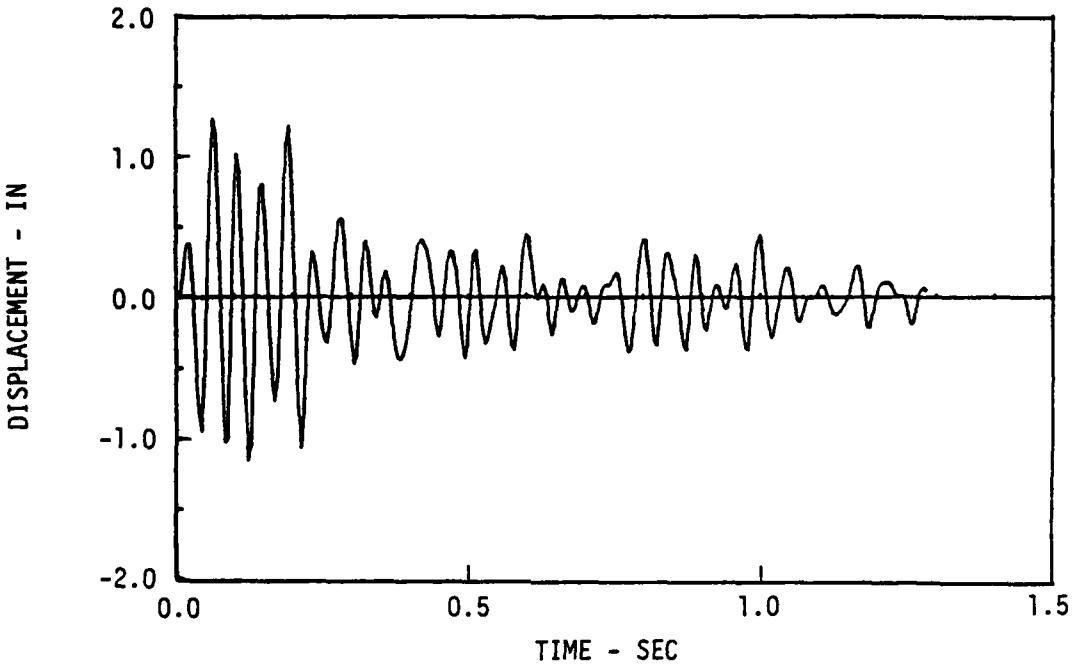

Figure 5.5a. Displacement response of identified system to force in Figure 5.1a. (Case 2)

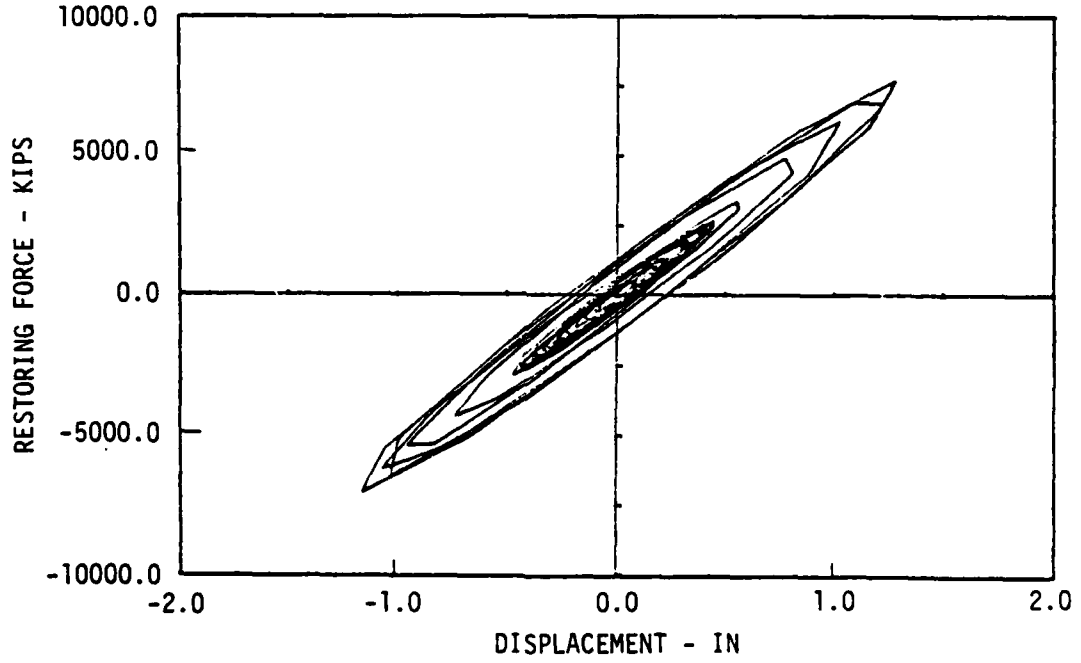

Figure 5.5b. Spring plus damper restoring force versus displacement for identified system. (Case 2)

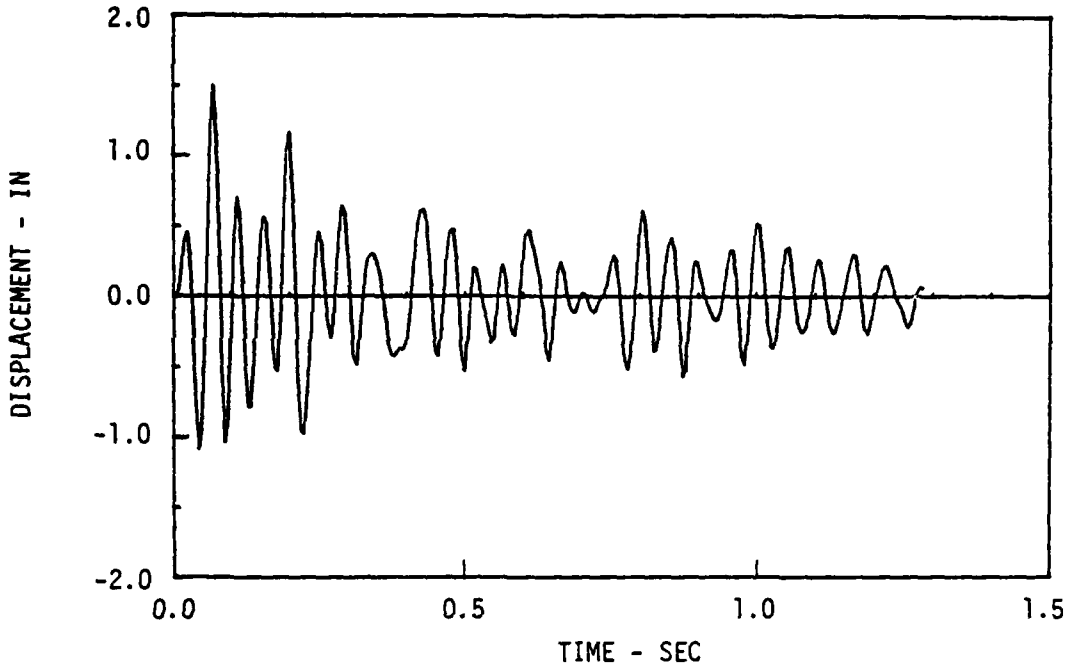

Figure 5.6a. Displacement response of identified system to force in Figure 5.1a. (Case 3)

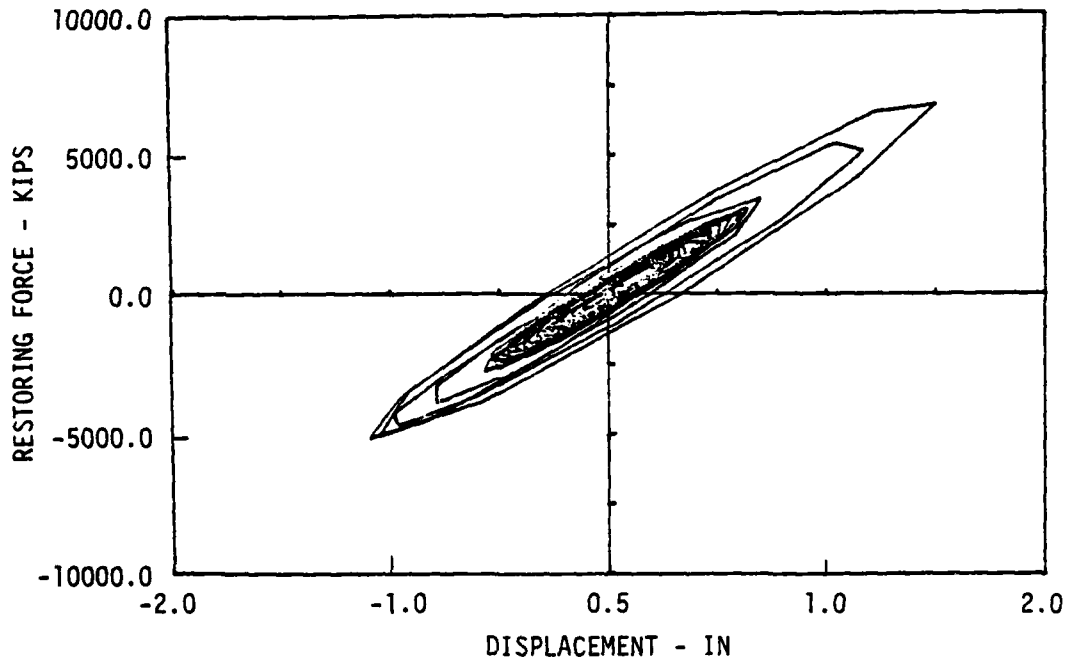

Figure 5.6b. Spring plus damper restoring force versus displacement for identified system. (Case 3)

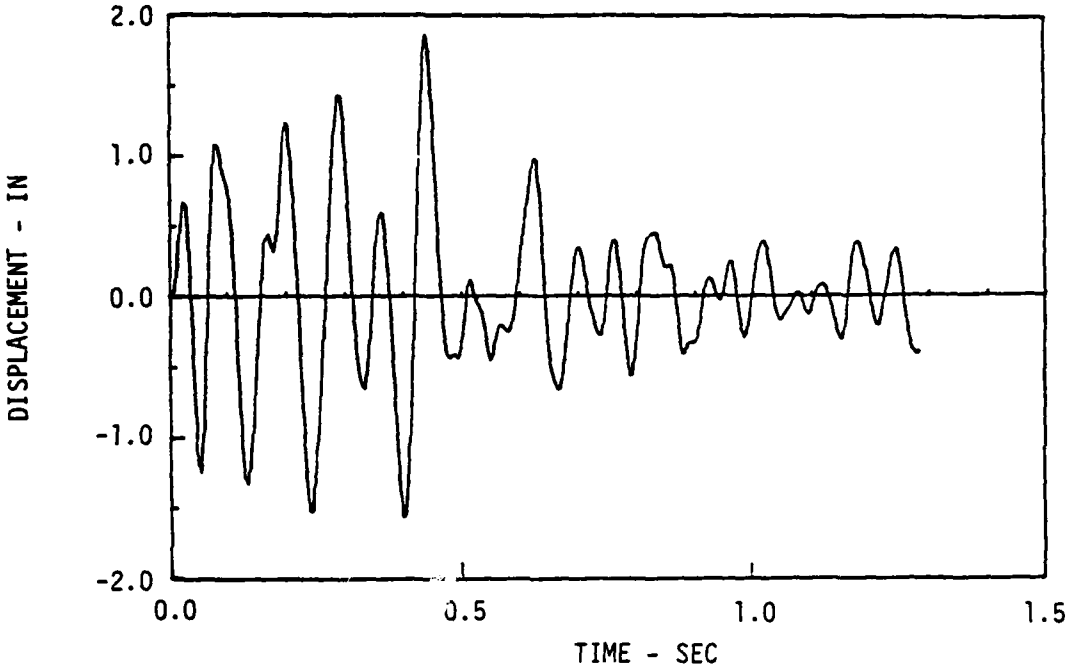

Figure 5.7a. Displacement response of identified system to force in Figure 5.1a. (Case 4)

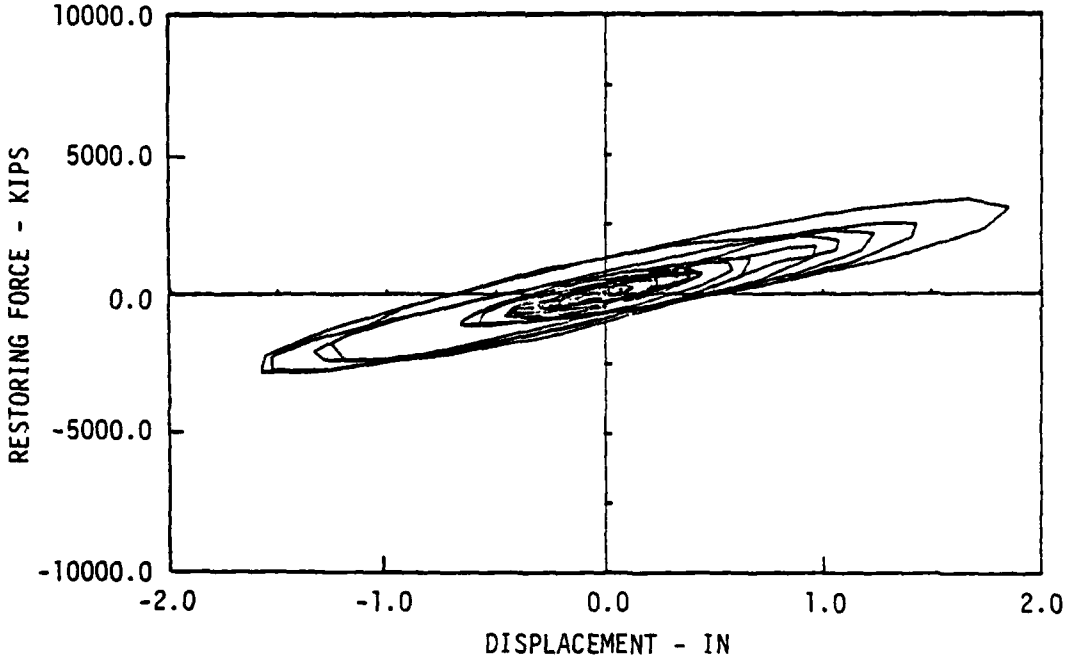

Figure 5.7b. Spring plus damper restoring force versus displacement for identified system. (Case 4)

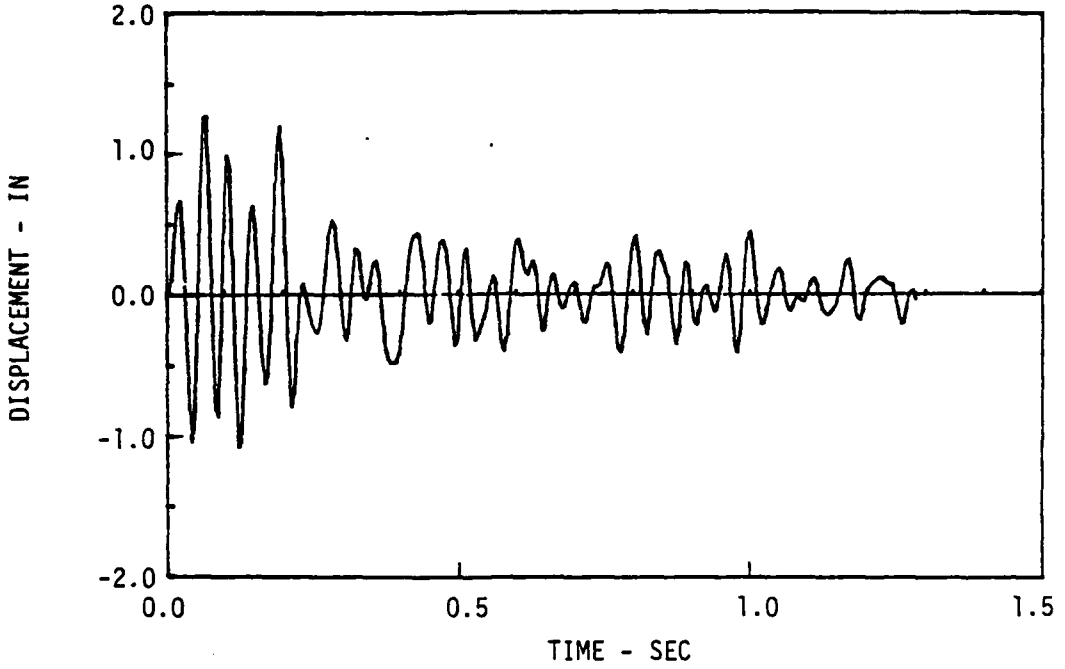

Figure 5.8a. Displacement response of identified system to force in Figure 5.1a. (Case 7)

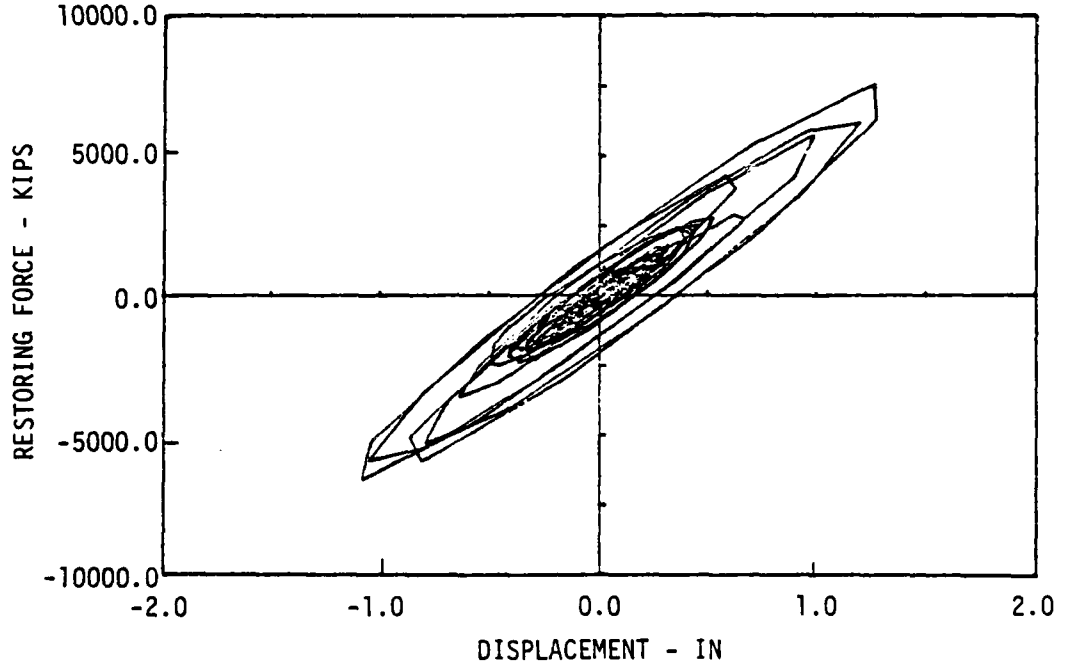

Figure 5.8b. Total restoring force versus displacement for identified system. (Case 7)

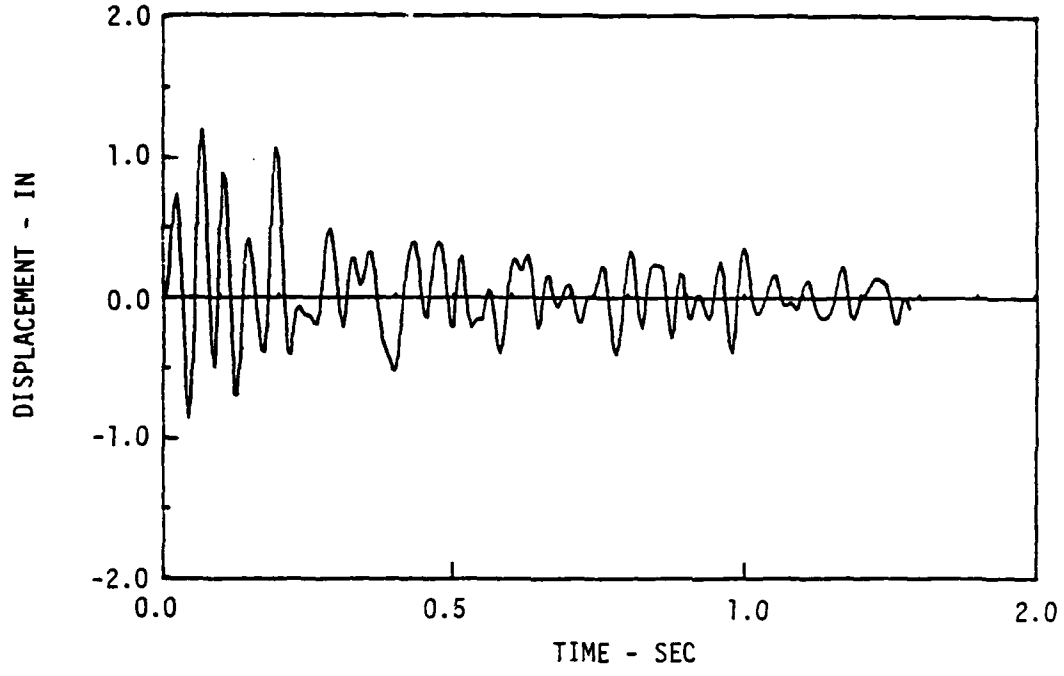

Figure 5.9a. Displacement response of identified system to force in Figure 5.1a. (Case 8)

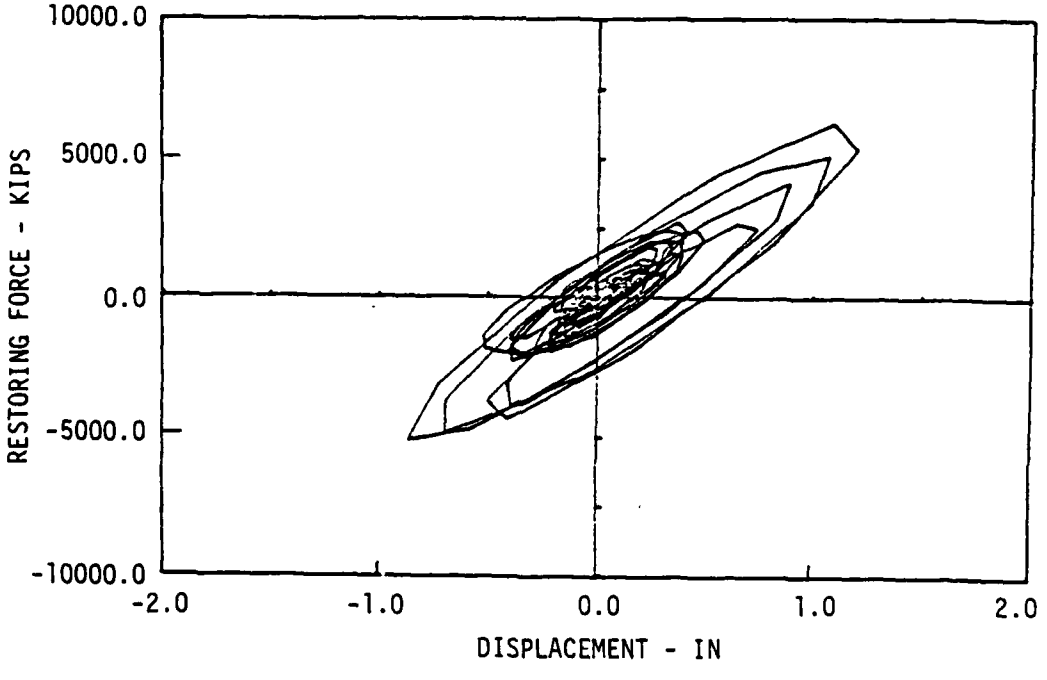

Figure 5.9b. Total restoring force versus displacement for identified system. (Case 8)

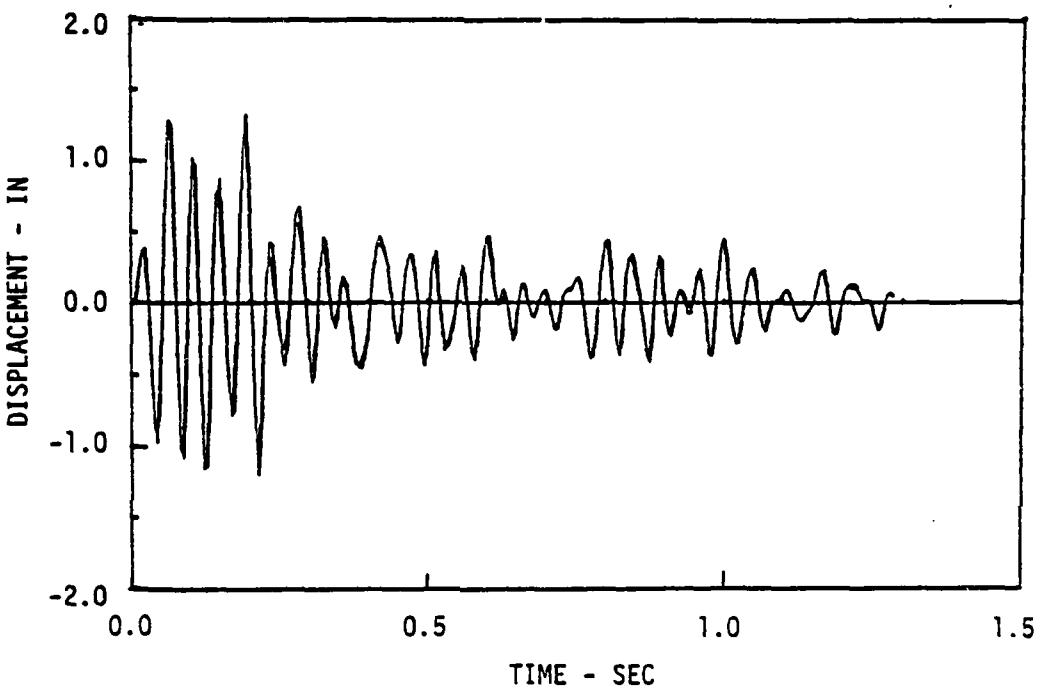

Figure 5.10. The comparison between measured response (light line) and identified response (dark line) for both second-order (case 3) and third-order (case 7) approximate systems. (The identified responses are practically the same.)

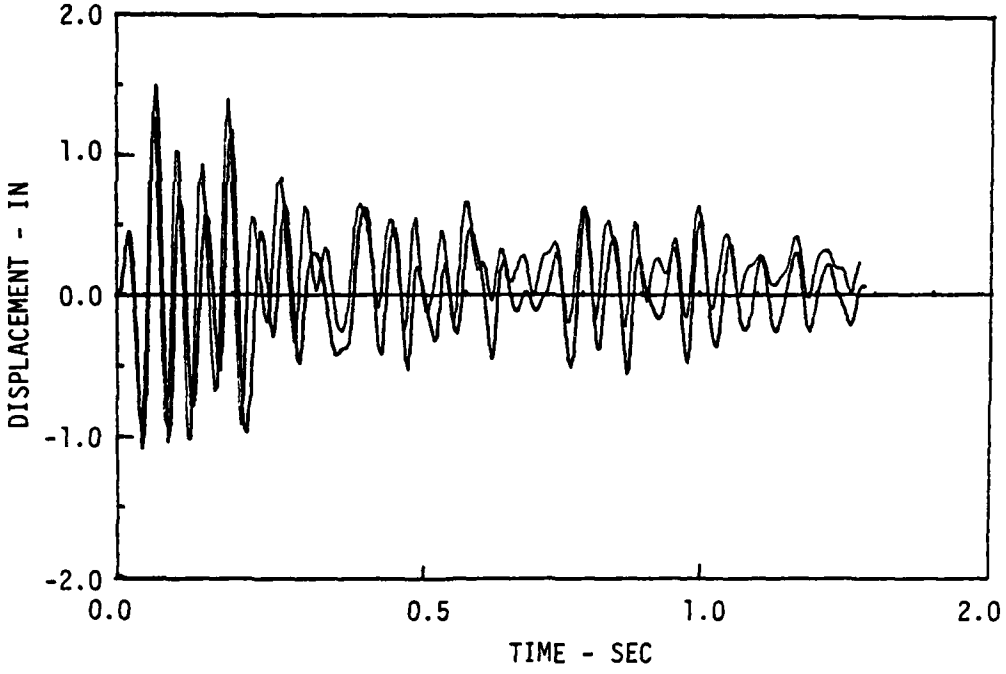

Figure 5.11a. The comparison between measured response (light line) and identified response for second-order system. (Case 3)

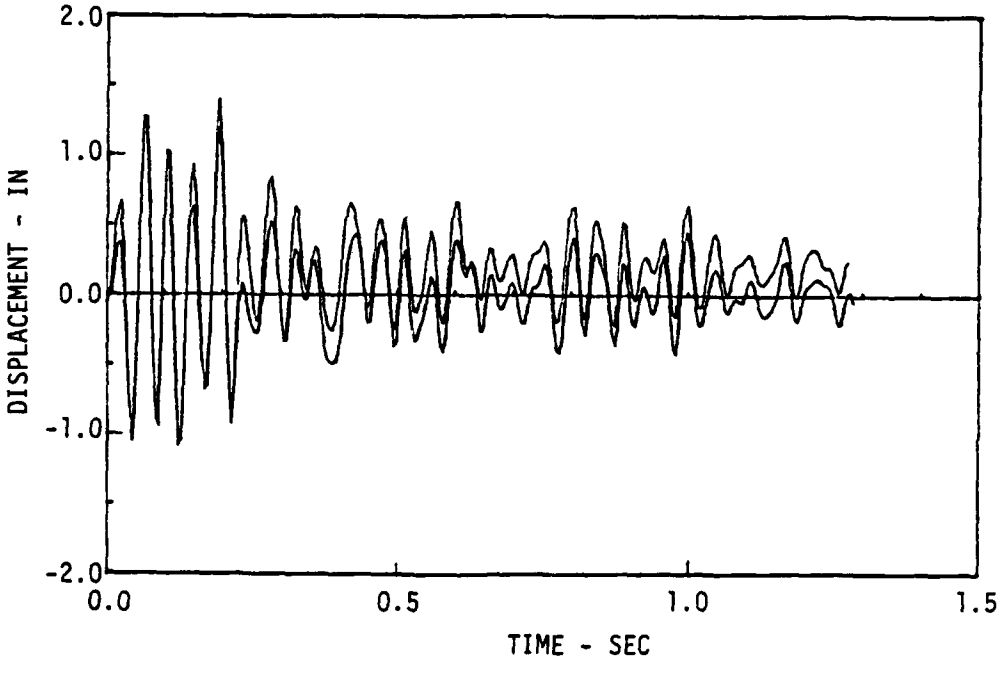

Figure 5.11b. The comparison between measured response (light line) and identified response for third-order system. (Case 7)

The numerical examples summarized here show that the direct, time domain parameter identification technique can be used effectively when the measured signals are noise free. This is best confirmed by reference to Figures 5.10, 5.11a, and 5.11b. These show that the linear model response can be made to match the nonlinear response well.

The energy dissipation results, summarized in Table 5.1, show that the third-order models provide the best simulation for a nonlinear hysteretic system.

5.2 Example 2

The parameter identification problem is solved in this example using the time domain approach with the integrated equation of motion. This approach was developed in Equations 3.13 through 3.18. The forcing function input used to excite the systems in this example is the same one used in Example 1. The forcing function parameters are listed in Table 5.2. In the present case, though, the time increment where the forcing function was evaluated is $\Delta t = 5 \times 10^{-5}$ sec. It was found, in working several numerical examples, that a time increment of extremely small magnitude, relative to the natural period of the system under investigation, is necessary to make the system identification work when noise is present in the inputs and outputs.

The structural systems analyzed in the 6 cases of the present numerical example are summarized in Table 5.2. The response of a linear system was computed for analysis in cases 1 and 4. The responses of moderately and strongly nonlinear systems were computed for analysis in cases 2 and 5 and cases 3 and 6, respectively.

In all cases in this numerical example, noise was added to the generated forcing function input and the measured acceleration response. The standard deviations of the band-limited, white noise, random processes added to the inputs and responses are given in Table 5.2. Figures 5.12a and 5.12b show segments of

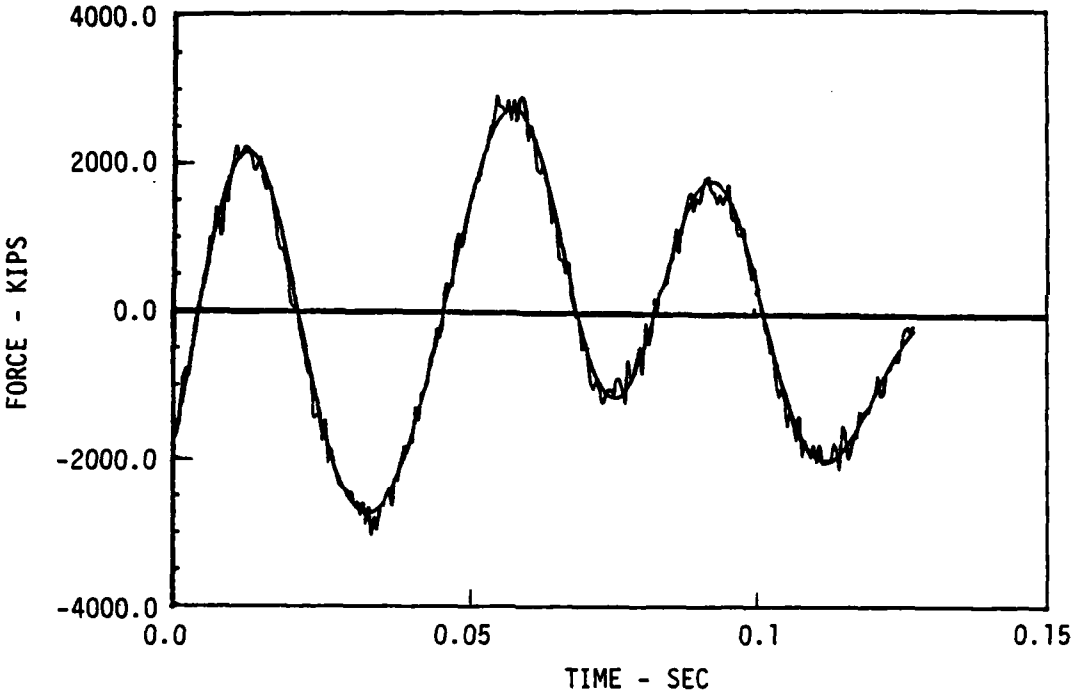

Figure 5.12a. Noisy and noise-free forcing function signals. The noisy signal is used in Example 2.

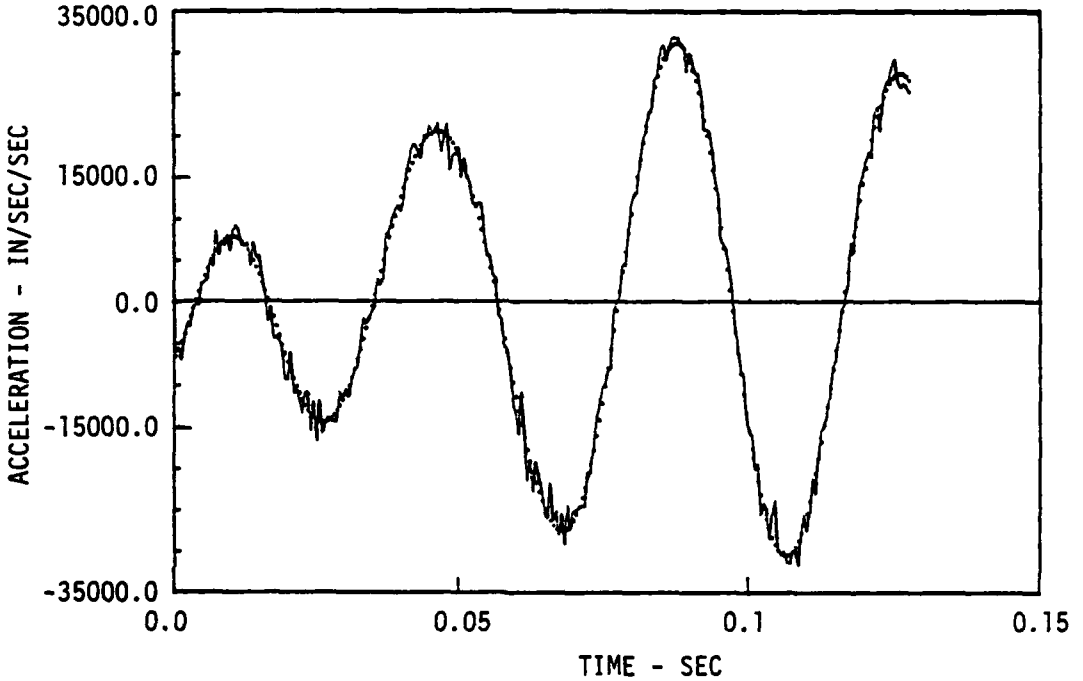

Figure 5.12b. Noisy and noise-free acceleration response signals. The noisy signal is used in Example 2.

Table 5.2. Parameters and Results for Example 2

Input (Structural Excitation)

Case Number	N	α	c	w_1	w_N	n	Δt
1 through 6	50	1.0	300	32.4	1256.4	256	5×10^{-5}

Structural Parameters

Case Number	m	c	k	k_y	z_y	E_D
1,4	0.259	7.77	5829	-	∞	22.7
2,5	0.259	7.77	5829	0	2000	22.7
3,6	0.259	7.77	5829	0	1000	22.7

Noise Parameters

Case Number	σ_f	σ_s
1 through 6	150	475

Identification Parameters and Results

Case Number	M	a_0	a_1	a_2	E_D
1	2	5809	7.89		22.8
2	2	4526	14.20		26.5
3	2	1563	18.19		24.6
4	3	5737	9.11	0	24.1
5	3	3851	70.79	0.00141	28.9
6	3	1056	18.50	0.00147	

the generated forcing function and the computed acceleration response with noise added. A typical segment of the white noise realization added to the input and response is shown, alone, in Figure 5.12c.

Parameter identifications were executed using the noisy inputs and responses summarized above. The results are listed at the bottom of Table 5.2. Comparison of the actual values for energy dissipated and the identified values for energy dissipated, in Table 5.2, shows that the identified models provide a reasonable estimate for energy dissipated in the actual system.

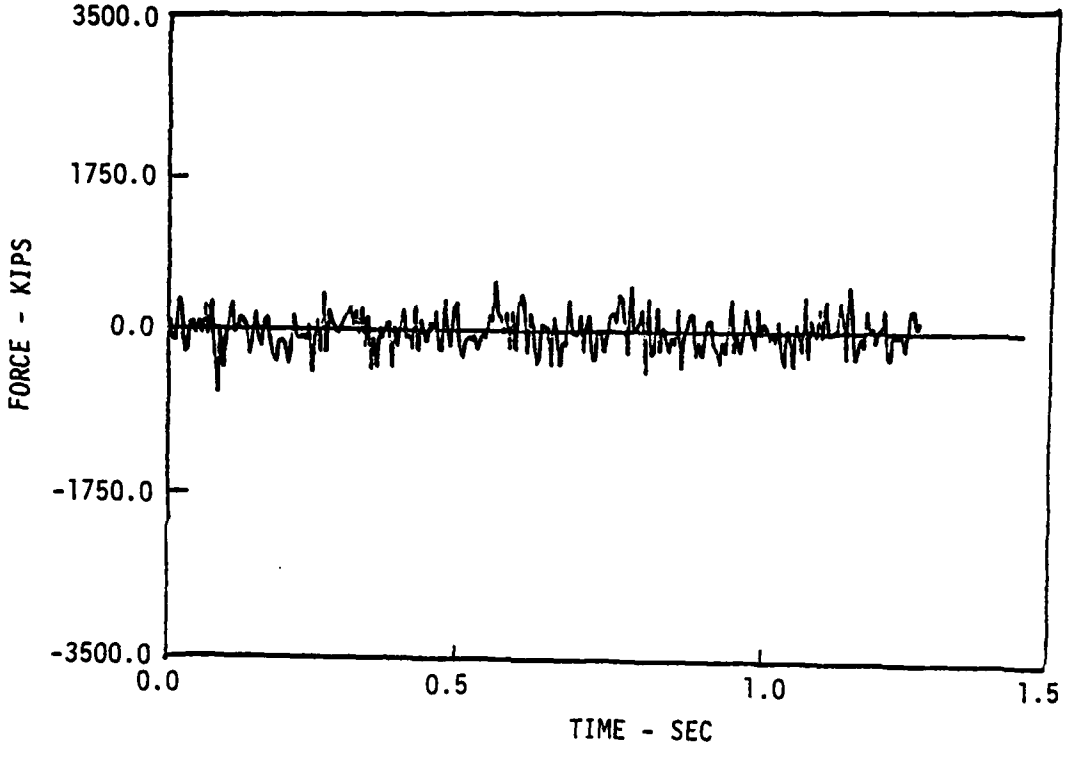

Figure 5.12c. Typical white noise signal used in numerical examples

The capability to establish such an estimate in the presence of noise provides an improvement over the parameter identification method used in Example 1.

5.3 Example 3

In this example, a parameter identification problem is solved using the frequency domain approach, developed in Equations 3.19 through 3.41. The shock input used in this example is a decaying exponential, oscillatory input. The input parameters are listed in Table 5.3. These parameters are the same for all eight cases worked in this example. A forcing function generated using the Table 5.3 parameters is shown in Figure 5.13a. Parameter identifications were performed both when noise was and was not present on the forcing function input. The standard deviations of the noise random processes for all eight cases worked in this example are listed in Table 5.3. Note that cases 2, 4, 6 and 8 are noisy; cases 1, 3, 5 and 7 are not noisy. The forcing function input with a white noise superimposed on it is shown in Figure 5.13b.

Two structural responses to the input of Figure 5.13a were computed. The first response was for a linear, SDF system; the structure parameters are listed in Table 5.3. This response was used in example cases 1, 2, 5 and 6. The second response was for a bilinear hysteretic system; the structural parameters are listed in Table 5.3. This response was used in example cases 3, 4, 7 and 8. The acceleration response of the nonlinear system is shown in Figure 5.14a. Parameter identifications were performed both when noise was and was not present on the acceleration response. The standard deviations of the white noise random processes are listed in Table 5.3 for all 8 cases. Figure 5.14b shows the nonlinear acceleration response from Figure 5.14a with a measurement white noise superimposed. Figure 5.15 shows the graph of restoring force (spring plus damper forces) versus displacement.

Table 5.3. Parameters and Results for Example 3

Input (Structural Excitation)

Case Number	N	α	c	w_1	w_N	n	Δt
1 through 8	50	0.025	1.0	0.8	1.2	1024	0.3

Structure Parameters

Case Number	m	c	k	k_y	z_y	z_{max}	E_D
1,2	1.0	0.2	1.0	-	∞	12.5	513.1
3,4	1.0	0.2	1.0	0.5	10.0	12.7	532.6
5,6	1.0	0.2	1.0	-	∞	12.5	513.1
7,8	1.0	0.2	1.0	0.5	10.0	12.7	532.6

Noise Parameters

Case Number	σ_f	σ_s
1	0.0	0.0
2	0.2	0.5
3	0.0	0.0
4	0.2	0.5
5	0.0	0.0
6	0.2	0.5
7	0.0	0.0
8	0.2	0.5

Identification Parameters and Results

Case Number	M	a_0	a_1	a_2	E_D
1	2	.9458	.1902		544.8
2	2	1.010	.2660		452.5
3	2	.9214	.1617		590.2
4	2	.9074	.1374		644.1
5	3	.9458	.3116	.08083	501.9
6	3	.9270	.2825	.06461	519.6
7	3	.9214	.2293	.02744	543.1
8	3	.9074	.2196	.02430	554.6

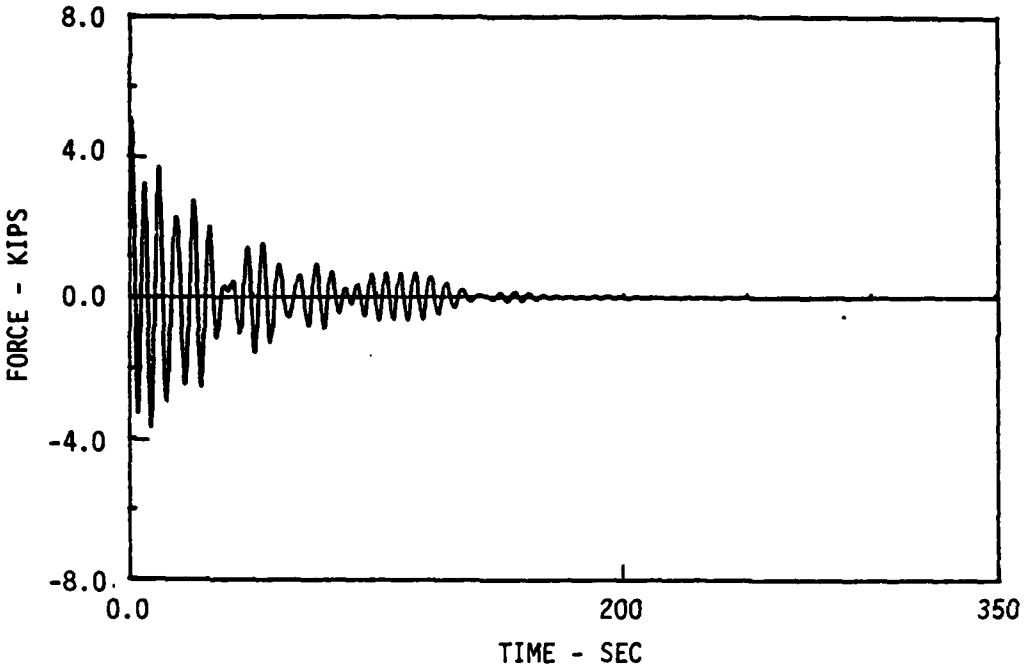

Figure 5.13a. Signal used to simulate the actual forcing function for an SDF system in Example 3

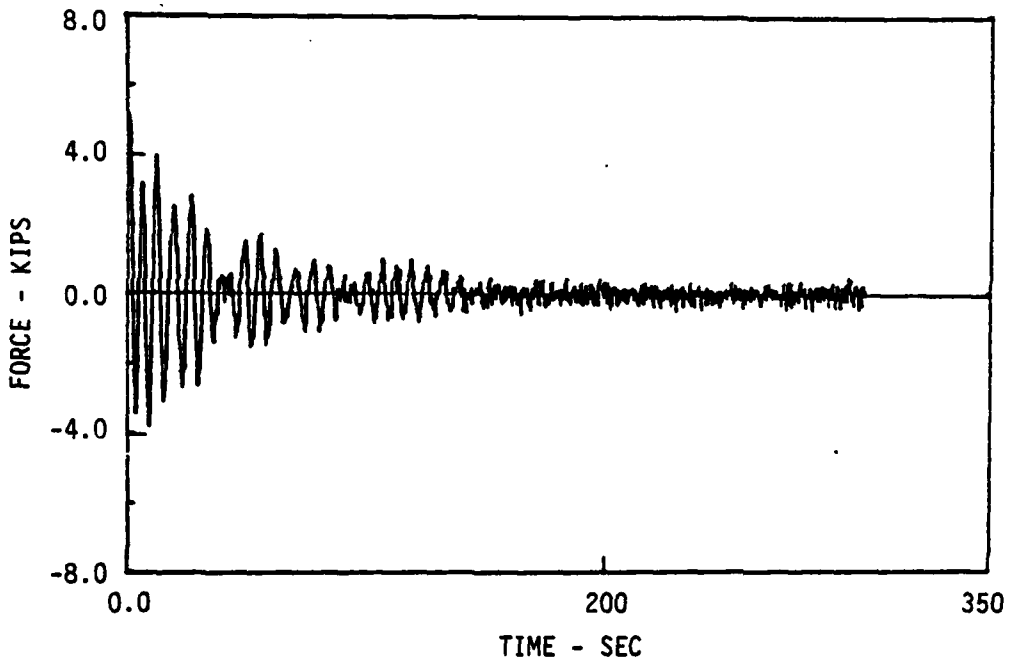

Figure 5.13b. Signal used to simulate the measured forcing function for an SDF system. (Includes noise.)

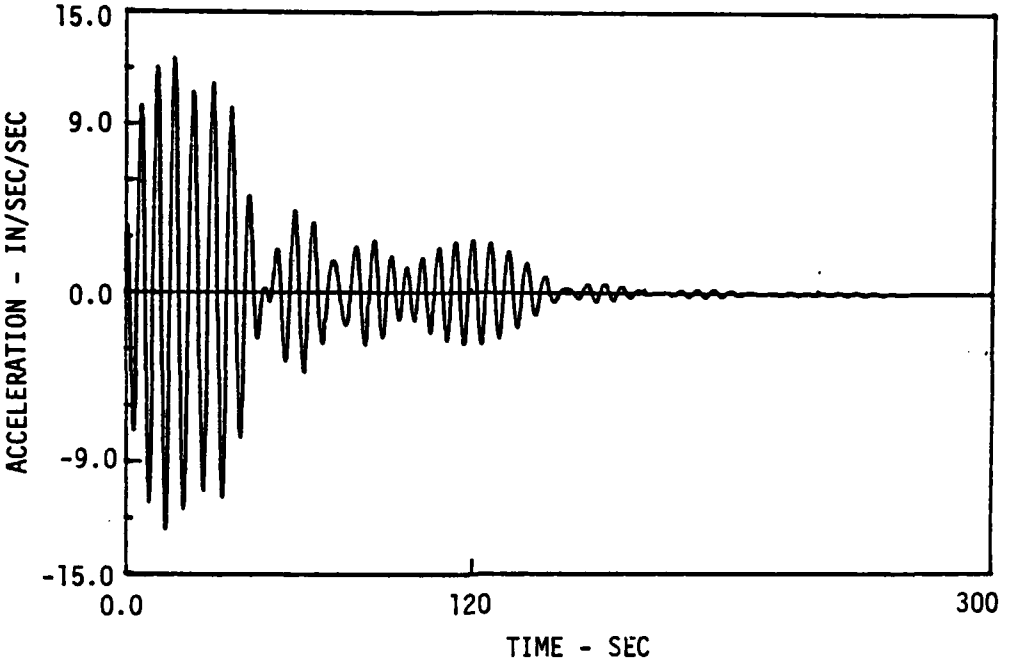

Figure 5.14a. Acceleration response of nonlinear SDF system to force in Figure 5.13a

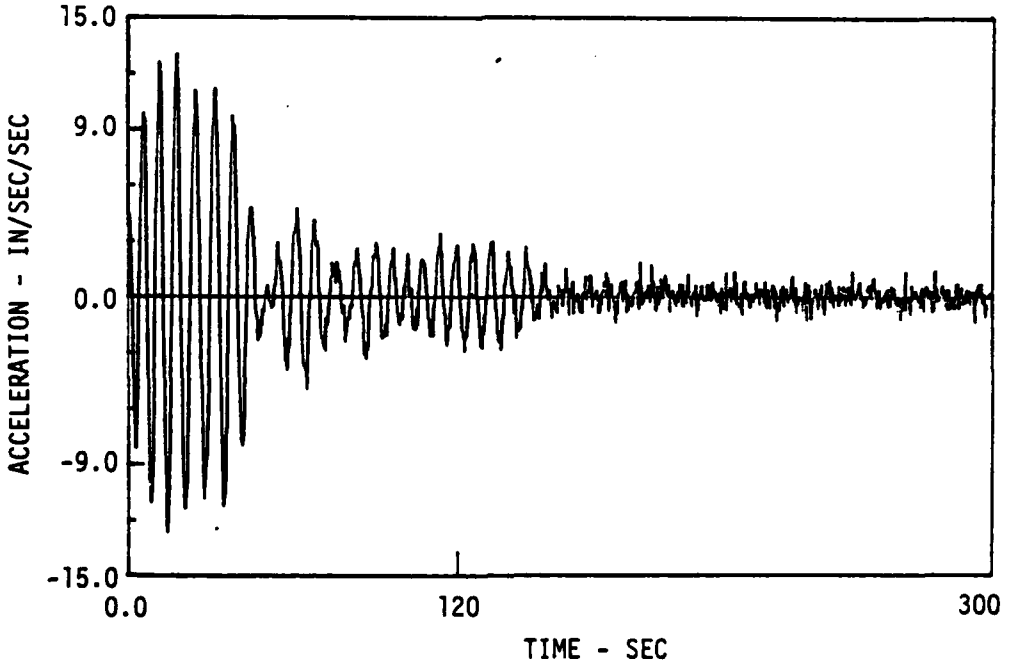

Figure 5.14b. Signal used to simulate measured acceleration response. Signal of Figure 14a plus noise.

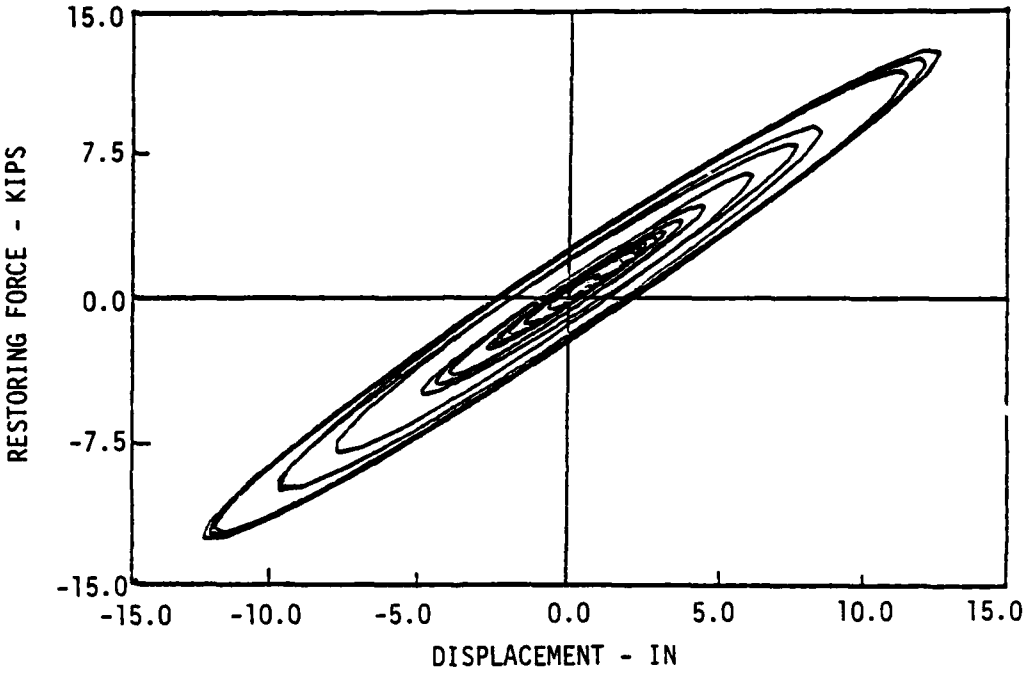

Figure 5.15. Total restoring force of nonlinear system versus displacement. (Cases 3, 4, 7 and 8)

The energy dissipated by the structure in each case of the numerical example is listed in Table 5.3 under the heading "Structural Parameters."

Parameter identifications were performed for the eight cases described above. The identified parameters are listed at the bottom of Table 5.3. The energy dissipated by each of the identification systems is listed next to the identified parameters.

Figures 5.16a and 5.16b show comparisons of the responses computed from the identified linear models to the nonlinear response of cases 3, 4, 7 and 8. Figure 5.16a compares the second-order model (M=0) response to the actual response. Figure 5.16a compares the third-order model (M=1) response to the actual response. The plots show that the third-order model provides a better visual match to the actual response than the second-order model. However, both linear models provide a good simulation of the nonlinear response.

Figures 5.16a and 5.16b make it apparent that the frequency domain parameter identification technique provides acceptable results, at least in those cases considered here.

The results show that the third-order model is preferable to the second-order model for estimation of the energy dissipated by the nonlinear response.

6.0 Discussion and Conclusions

The main objective of this investigation was to establish a method for measuring the damage accumulation in structures. We assumed that structural damage is related to the energy dissipated during a strong motion event and attempted to identify this quantity.

The estimate for energy dissipated by a structure was obtained by identifying the parameters for a model of the damaged structure, then using the model to compute the energy dissipated during the strong motion event. The model chosen to simulate the

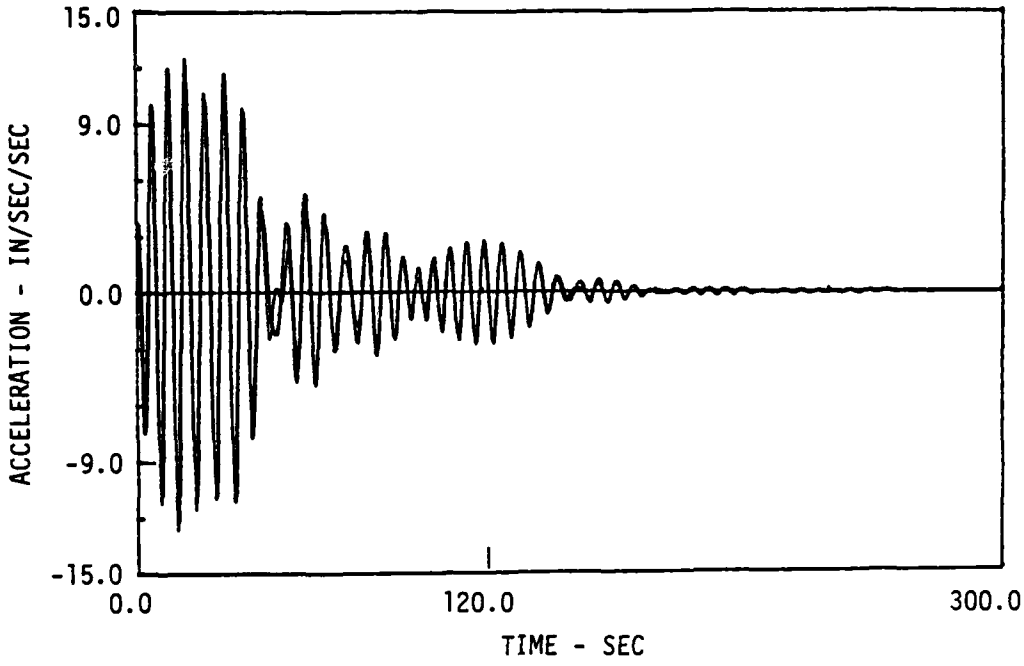

Figure 5.16a. The comparison between noise-free response (light) and third-order identified response. (Parameters from case 8)

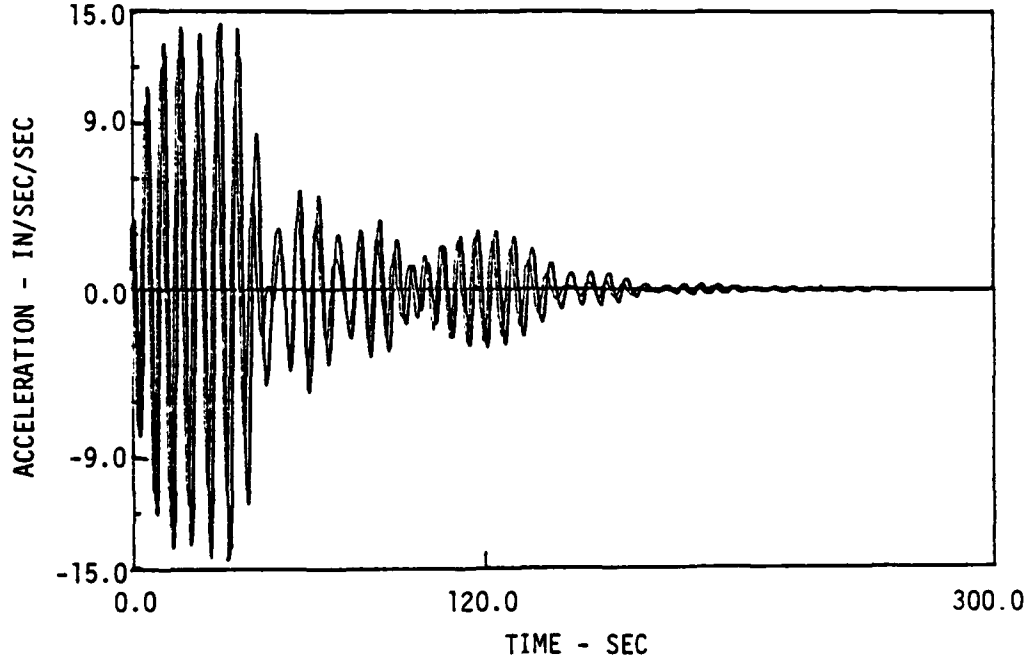

Figure 5.16b. The comparison between noise-free response (light) and second-order identified response. (Parameters from case 4)

response of the damaged structure is a system of linear differential equations. Specifically, second- and third-order, linear, ordinary, differential equations were used to model the motions of single-degree-of-freedom (SDF) hysteretic systems.

The parameters of the model were estimated using three approaches. Two of these approaches are time domain least squares approaches where the modeling error is minimized with respect to the measured data. The other is a frequency domain least squares approach.

Many numerical examples were solved, and some of them are summarized in this report. Experience obtained in solving the numerical examples leads to the following conclusions.

(1) Linear and nonlinear hysteretic single-degree-of-freedom (SDF) system responses can be accurately modeled using second- and third-order linear equations.

(2) A direct, time domain approach can be used to identify model parameters when the force input and acceleration response measurements are not noisy.

(3) A time domain approach using integrated equations of motion can be used to identify model parameters when the input and response measurements are noisy. However, an accuracy requirement forcing Δt to be very small when this approach is used reduces the effectiveness of this method.

(4) A frequency domain approach to the identification of SDF system parameters is most effective in the present application. It can be used when measurement noise is present in the input and response and leads to accurate results.

(5) The third-order, linear model is preferable to the second-order model in at least two respects. 1) The third-order model provides a better match to the nonlinear SDF system response than the second-order

model. 2) The third-order model provides a better estimate of energy dissipated by the nonlinear system than the second-order model.

The present approach to frequency domain parameter identification and estimation of energy dissipated by a hysteretic SDF system yields accurate results. However, the degree of accuracy in the present analysis can be improved. In particular, the present analytical approach would be improved by introduction of a numerical search procedure for location of the system parameters which correspond to a least squares solution. Such a change in the analysis would eliminate the need for the simplifying assumptions used in this study.

Future investigations should attempt to improve the models established in this study and consider more complicated systems. The models considered in this study can be made more elaborate and, possibly, more accurate. For example, linear models with time varying parameters can be considered; and nonlinear models can be considered. (The drawback in the use of nonlinear models is that the frequency domain analysis can no longer be used.) The analysis of energy dissipated in two-degree-of-freedom structures should be pursued.

Future studies should include numerical examples of error analysis. The present investigation derived the equations for error analysis, but no numerical computations of confidence intervals were included in the examples.

ACKNOWLEDGEMENT

This study was funded by the Air Force Office of Scientific Research under contract number 81-0086. The authors gratefully acknowledge this support.

REFERENCES

1. Wen, Y. K., "Stochastic Response Analysis of Hysteretic Structures," Proceedings of the Specialty Conference on Probabilistic Mechanics and Structural Reliability, ASCE, Tuscon, Arizona, January, 1979.

2. Baber, T. T. and Wen, Y. K., "Equivalent Linearization of Hysteretic Structures," Proceedings of the Specialty Conference on Probabilistic Mechanics and Structural Reliability, ASCE, Tuscon, Arizona, January, 1979.

3. Baber, T. T. and Wen, Y. K., "Random Vibration of Hysteretic, Degrading Systems," Journal of the Engineering Mechanics Division, ASCE, Vol. 7, No. EM6, December, 1981.

4. Lutes, L. D. and Hsieh, J., "Higher Order Equivalent Linearization in Random Vibration," Proceedings, Third Engineering Mechanics Division Specialty Conference, ASCE, Austin, Texas, September, 1979.

5. Wafa, F., Peak Response of Hysteretic Structures, Ph.D. Dissertation, Department of Civil Engineering, University of New Mexico, Albuquerque, N.M., August, 1981.

6. Raiffa, H. and Schlaifer, R., Applied Statistical Decision Theory, Harvard University, Division of Research, Harvard Business School, Boston, 1961.

7. Newland, D. E., An Introduction to Random Vibrations and Spectral Analysis, Longman, London, 1975.

8. Clough, R. W. and Penzien, J., Dynamics of Structures, McGraw-Hill, 1975.

ATE
LME
8